

Non-conventional Behavior of a 2,1-Benzazaphosphole: Heterodiene or Hidden Phosphinidene?

Vít Kremláček,^[a] Erik Kertész,^[b] Zoltán Benkő,^{*,[b]} Milan Erben,^[a] Robert Jirásko,^[c] Aleš Růžička,^[a] Roman Jambor,^[a] and Libor Dostál^{*,[a]}

Abstract: The titled 2,1-benzazaphosphole (1) (i.e. ArP, where Ar=2-(DippN=CH)C₆H₄, Dipp=2,6-*i*Pr₂C₆H₃) showed a spectacular reactivity behaving both as a reactive heterodiene in hetero-Diels-Alder (DA) reactions or as a hidden phosphinidene in the coordination toward selected transition metals (TMs). Thus, 1 reacts with electron-deficient alkynes RC≡CR (R=CO₂Me, C₅F₄N) giving 1-phospha-1,4-dihydro-iminonaphthalenes 2 and 3, that undergo hydrogen migration producing 1-phosphanaphthalenes 4 and 5. Compound 1 is also able to activate the C=C double bond in selected *N*-alkyl/aryl-

maleimides RN(C(O)CH)₂ (R=Me, *t*Bu, Ph) resulting in the addition products 7–9 with bridged bicyclic [2.2.1] structures. The binding of the maleimides to 1 is semi-reversible upon heating. By contrast, when 1 was treated with selected TM complexes, it serves as a 4e donor bridging two TMs thus producing complexes [μ-ArP(AuCl)₂] (10), [(μ-ArP)₄Ag₄][X]₄ (X=BF₄ (11), OTf (12)) and [μ-ArP(Co₂(CO)₆] (13). The structure and electron distribution of the starting material 1 as well as of other compounds were also studied from the theoretical point of view.

Introduction

Monomeric compounds (R–P), known as phosphinidenes,^[1] represent a very interesting group of neutral, electron deficient and highly reactive species. Their high reactivity is caused mainly by the fact that they often have a triplet ground state, for example for parent (H–P) the triplet state is by 20 kcal mol⁻¹ more stable than the singlet one.^[2] Therefore their stabilization is not trivial and they are often treated and studied as elusive and very reactive intermediates at low temperatures.^[3] They can also be generated in situ starting from suitable precursors relying on a coordination toward a transition metal (TM) fragment.^[4] Later on, Cummins et al. showed that phosphinidenes may be generated successfully from metal-free precursors as well and can be transferred to other substrates.^[5] The

majority of these processes is based on a re-aromatization and a thermal loss of anthracene or related aromatic compounds (Scheme 1A).

Theoretical studies showed that a presence of strongly π-donating substituents, such as R₂N– or R₂P–, attached directly to the phosphinidene center might efficiently stabilize singlet

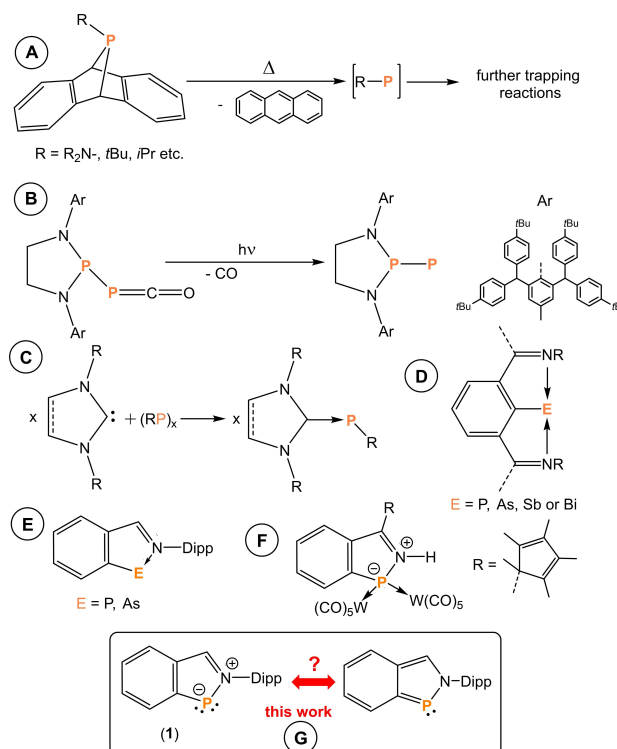
[a] V. Kremláček, M. Erben, Prof. A. Růžička, Prof. R. Jambor, Prof. L. Dostál
Department of General and Inorganic Chemistry
FCHT, University of Pardubice
Studentská 573, 532 10 Pardubice (Czech Republic)
E-mail: libor.dostal@upce.cz

[b] Mr. E. Kertész, Prof. Z. Benkő
Department of Inorganic and Analytical Chemistry,
Budapest University of Technology and Economics
Szent Gellért tér 4, H-1111 Budapest (Hungary)
E-mail: zbenko@mail.bme.hu

[c] R. Jirásko
Department of Analytical Chemistry
FCHT, University of Pardubice
Studentská 573, 532 10 Pardubice (Czech Republic)

Supporting information for this article is available on the WWW under
<https://doi.org/10.1002/chem.202101686>

© 2021 The Authors. Chemistry - A European Journal published by Wiley-VCH GmbH. This is an open access article under the terms of the Creative Commons Attribution Non-Commercial NoDerivs License, which permits use and distribution in any medium, provided the original work is properly cited, the use is non-commercial and no modifications or adaptations are made.



Scheme 1. Relevant pnictinidene-like systems for this study.

phosphinidenes.^[6] This strategy in combination with a sufficient steric shielding allowed the isolation of the first monomeric bottle-able (phosphino)phosphinidene (Scheme 1B) that was synthesized from a bulky (phosphino)phosphaketene by the group of Bertrand.^[7] Its phosphinidene-character was also proven by subsequent reactivity studies.^[8]

Another approach for the stabilization of monomeric singlet phosphinidenes involves their coordination by a Lewis base, that completes the octet at the phosphorus atom, thereby stabilizing the singlet state. Since the appearance of the first examples synthesized by a disintegration of (RP)_n cycles employing N-heterocyclic carbenes (NHCs)^[9] (Scheme 1C), this family of compounds became popular and this field has already been reviewed. The structure of these compounds is often on the border between coordinated phosphinidenes and phosphalkenes depending on the particular carbene used.^[11,10]

We and others have demonstrated that *N,C,N*-pincer ligands are able to stabilize monomeric pnictogen(I) compounds (Scheme 1D).^[11] Later on, it turned out that for the lighter elements (Scheme 1E) one pendant imino- functionality is sufficient enough to stabilize given monomeric species,^[12,13] while in the case of the antimony and bismuth analogues oligomers or unstable compounds were obtained instead.^[14] It is also to note that a structurally related azaphosphole has been isolated as a complex with two W(CO)₅ groups (Scheme 1F).^[15]

Compound **1** revealed a very short P–N bond distance and exhibited significant aromatic character based on NICS values and ACID analysis, therefore it may also be regarded as a 2,1-benzazapnictole (Scheme 1G).^[11] Recently, the pronounced heterodiene-character of these compounds has been demonstrated on their reactivity toward electron deficient alkynes that proceeded as a hetero Diels-Alder (DA) reaction.^[16]

This study aims to examine the reactivity of the titled 2,1-benzazaphosphole (**1**). Based on a thorough theoretical study reported herein (see below), it is expected to exhibit a spectacular dual chemical behavior serving as a heterodiene or playing the role of a hidden phosphinidene (**G**). To prove this hypothesis, the reactivity of **1** toward electron deficient dienophiles and selected TM complexes is reported.

Results and Discussion

Theoretical considerations

In order to explore the electronic structure of compound **1**, we carried out density functional calculations at the ω B97XD/def2-TZVP level (a similar level of theory has been employed for other azaphospholes^[17]) and we performed Natural Bond Orbital (NBO) analysis including Natural Resonance Theory (NRT) analysis to describe the possible resonance structures. Furthermore, to gain insights into the bonding situations, Wiberg Bond Indices (WBI) and the Natural Population Analysis (NPA) charges were obtained. In the following we only discuss the parent compound (H substituent at the nitrogen in the following shown as **1'**), but for the Dipp substituted analogue similar

conclusions can be deduced (see of Table 1 and Table S2 for details).

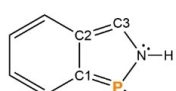
To describe the bonding and charge distribution in the model benzazaphosphole **1'**, we studied the relevance of the resonance structures obtained from the NRT-analysis (Scheme 2).

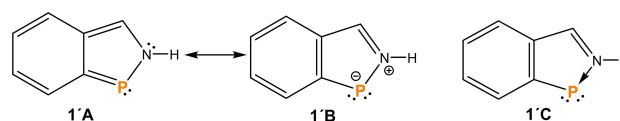
This resulted in various resonance structures, and only two resonance structures have weights above 10%: **1'A** and **1'B** with 17.1% and with 12.5% weights, respectively. Note that the further resonance structures having even lower weights represent unusual delocalization (e.g. negative charge at the carbon centers) and thus are not discussed. Resonance structure **1'A** exhibits a P=C double bond and one lone pair of electrons at the phosphorus center as well as two C=C double bonds toward the anellation. In contrast, in the zwitterionic resonance structure **1'B** the P center possesses two lone pairs and thus a negative charge as well as a C=N⁺ double bond. **1'C** shows an alternative representation to resonance structure **1'B** with an N→P dative bond instead of the N⁺–P[–] zwitterion (in analogy with H₃N→BH₃ vs. NH₃⁺–BH₃[–]). As their meaning is similar, in the following we will use **1'B**. (Note that resonance theory does not consider the dative bond as depicted in **1'C**, and strictly, only the structure **1'B** could be obtained in the NRT analysis.)

The bond distances and Wiberg Bond Indices (WBIs) further support the relevance of the two leading resonance structures (Table 1). The P–N bond in the five-membered ring can be described as a single bond (WBI=0.96, for H₂N–PH₂: WBI=0.93), but the remaining C–N and C–C bonds show significant and extended π -delocalization (WBI=1.23–1.37). To further interpret the WBIs, we compared them with an appropriate (hypothetical) reference compound: H₂C=P–NHMe, in which the P–N bond has a WBI of 0.91, while the P=C bond of 1.77. Indeed, the WBI of the C1=P bond in the benzazaphosphole **1'** (WBI=1.29) indicates remarkable delocalization compared to the localized C=P bond (WBI=1.77) in H₂C=P–NHMe.

Furthermore, the relevance of the resonance structure **1'B** is also bolstered by the NPA-charges. In comparison with H₂C=P–NHMe (*q*(P)=0.908 e[–] and *q*(N)=–0.921 e[–]), in benzazaphosphole **1'** the P center is less positive (*q*(P)=0.623 e[–]), and the N center is significantly less negative (*q*(N)=–0.741 e[–]). Nevertheless, the charges are determined by both inductive

Table 1. Selected bond distances (*d*, [Å]) and Wiberg Bond Indices (WBI) at the ω B97XD/def2-TZVP level.

	Bond	<i>d</i> [Å]	WBI
	P–N	1.703	0.96
	P–C1	1.736	1.29
	N–C3	1.342	1.29
	C1–C2	1.430	1.23



Scheme 2. Leading resonance structures of compound **1'**.

and mesomeric effects, thus altogether the N atom possesses a negative, while the P atom a positive partial charge.

On the basis of the resonance structure **1'A** a reactivity in Diels-Alder reaction can be foreseen, and the resonance structure **1'B** hints for (double) complexation. The HOMO and the LUMO of benzazaphosphole **1'** (Figure 1) clearly indicate the ability for cycloadditions, because the HOMO orbital is located at the P and C₃ centers in opposite phase, thereby it can lead to a stabilizing interaction with an π^* type orbital of a

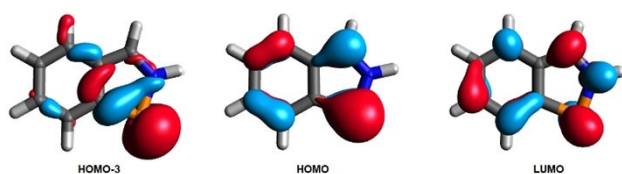
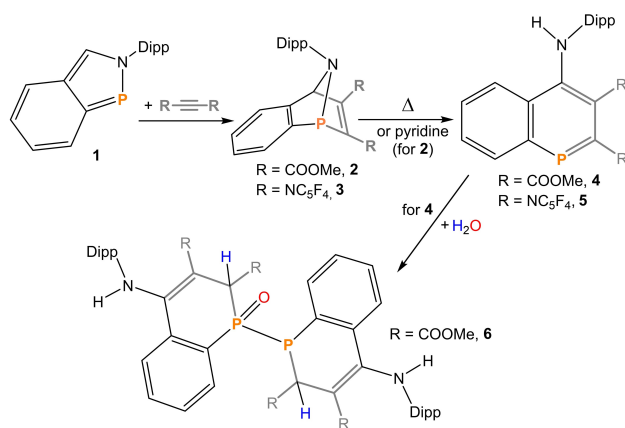


Figure 1. Selected Kohn-Sham orbitals of the model species **1'** at the ω B97XD/def2-TZVP level with a contour value of 0.05.



Scheme 3. Synthesis of compounds **2-6**.

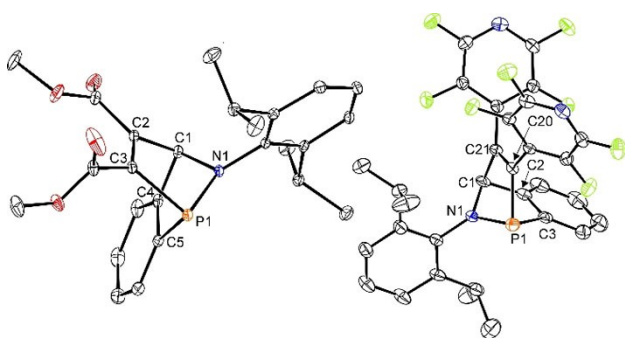


Figure 2. ORTEP presentation of the molecular structures of **2** (left) and **3** (right) (40% probability displacement ellipsoids). Hydrogen atoms and the alkyne co-crystallized molecule in the case of **3** are omitted. Bond lengths [Å] and angles [°] for **2**: P(1)–N(1) 1.704(2), P(1)–C(3) 1.904(2), P(1)–C(5) 1.854(2), N(1)–C(1) 1.478(2), C(1)–C(2) 1.545(2), C(2)–C(3) 1.331(2), C(1)–C(4) 1.529(2), C(4)–C(5) 1.401(3), N(1)–P(1)–C(5) 87.89(8), N(1)–P(1)–C(3) 88.65(7), C(3)–P(1)–C(5) 89.43(7). **3**: P(1)–N(1) 1.710(2), P(1)–C(3) 1.865(2), P(1)–C(20) 1.897(2), N(1)–C(1) 1.470(3), C(1)–C(2) 1.540(3), C(2)–C(3) 1.400(3), C(1)–C(21) 1.557(3), C(20)–C(21) 1.336(3), N(1)–P(1)–C(3) 88.44(10), N(1)–P(1)–C(20) 86.48(9), C(3)–P(1)–C(4) 90.12(9).

dienophile. On the other hand, in the LUMO these lobes are in the same phase, hence it can interact with the bonding π type orbital of a dienophile.

Moreover, the complex formation reactivity of compound **1'** can also be proposed on the basis of the HOMO-3 and HOMO molecular orbitals. The HOMO-3 orbital is mainly a P centered lone pair of high *s*-character, while the HOMO is a π orbital with extended delocalization, in which a large contribution of a *p*-type orbital can be found at the P center.

Reactivity of **1** as a heterodiene

Compound **1** reacted as a heterodiene in DA reactions^[18] with alkynes $RC\equiv CR$ ($R=CO_2Me$, C_5F_4N) under the formation of 1-phospha-1,4-dihydro-iminonaphthalenes **2** and **3** (Scheme 3). Their structures were unambiguously established by single crystal X-ray diffraction analysis (Figure 2). Compound **3** forms co-crystals with the starting alkyne.^[19]

The addition of the alkyne to **1** resulted in the formation of two new covalent bonds, i.e. P1–C3/20 (1.904(2) and 1.897(2) Å) and C1–C2/21 (1.545(2) and 1.557(3) Å, **2** and **3**, respectively) and all values correspond to the sum of covalent radii (cf. $\Sigma_{cov}(P-N)=1.82$ Å, $\Sigma_{cov}(P-C)=1.86$ Å and $\Sigma_{cov}(C-C)=1.50$ Å^[20]). The C2(20)–C3(21) bond lengths (1.331(2) and 1.336(3) Å) are indicative of the expected double character ($\Sigma_{cov}(C=C)=1.34$ Å^[21]). The $^{31}P\{^1H\}$ NMR spectra of **2** and **3** revealed one signal at $\delta(^{31}P)=39.9$ and 40.7 ppm both being significantly high-field shifted in comparison with **1** (182.8 ppm).^[12] The 1H and $^{13}C\{^1H\}$ NMR spectra also proved the presence of the *C(H)*NDipp group by typical signals at $\delta(^1H)=5.64$ and 5.26 ppm and at $\delta(^{13}C)=82.4$ and 84.4 ppm for **2** and **3**, respectively. Furthermore, two signals were obtained for the sp^2 carbon atoms of the $C=C$ bond resulting from the added alkyne (in the range 154.5–161.7 ppm for **2** and **3**).

Two infrared and Raman bands in the region 1729–1707 cm^{-1} indicate the presence of the carbonyl functions in **2**. A medium strength Raman band at 1610 cm^{-1} is assigned to the carbon-carbon double bond stretching of the added alkyne. Bands at ~ 1645 and ~ 1464 cm^{-1} corresponding to the tetrafluoropyridyl ring modes dominate the vibrational spectra of **3**; the $C=C$ bond stretching gives a Raman line at 1614 cm^{-1} .^[22]

Heating of **3** to 120 °C in toluene resulted in a hydrogen migration leading to 1-phosphanaphthalene **5** (Scheme 2). By contrast, analogous conversion of **2** to **4** solely by heating was very slow and accompanied by a gradual decomposition. Thus, a more convenient way of using pyridine as a hydrogen transfer agent^[23] was applied leading to a clean formation of **4** within 25 min at 55 °C (Figures S44–46). The molecular structure of **5** along with structural parameters is shown in Figure 3. By contrast all attempts to obtain single-crystals of **4** failed, but we have fortuitously obtained the structure of **6** (Scheme 3) as a product of an accidental hydrolysis^[24] (Figure 4).

The P1–C1(5) bond lengths (1.713(5) and 1.755(4) Å) in **5** are found between the expected values for a single and a double bond, respectively.^[20,21] These values are closely related to those

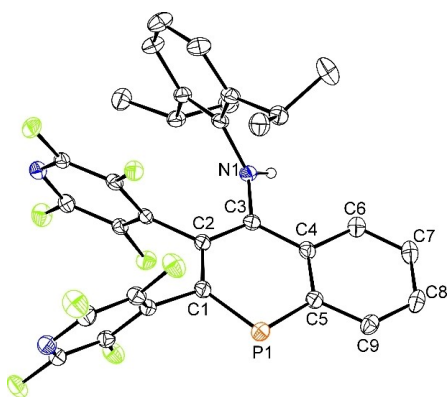


Figure 3. ORTEP presentation of the molecular structure of **5** (40% probability displacement ellipsoids). Hydrogen atoms except the NH group are omitted. Bond lengths [Å] and angles [°]: P(1)–C(1) 1.713(5), P(1)–C(5) 1.755(4), C(1)–C(2) 1.415(6), C(2)–C(3) 1.393(5), C(3)–C(4) 1.451(6), C(4)–C(5) 1.414(6), C(3)–N(1) 1.393(5), C(1)–P(1)–C(5) 100.4(2).

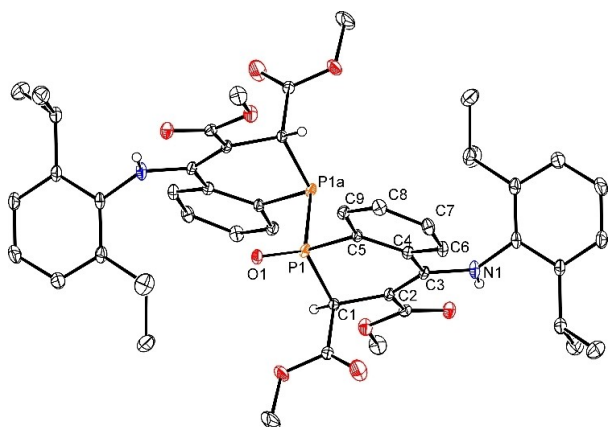


Figure 4. ORTEP presentation of the molecular structure of **6** (40% probability displacement ellipsoids). Hydrogen atoms except the relevant CH, and NH group and benzene solvent molecule are omitted. Symmetry operator $a = 1 - x, 1 - y, 1 - z$. Bond lengths [Å] and angles [°]: P(1)–P(1a) 2.209(7), P(1)–O(1) 1.426(3), P(1)–C(1) 1.837(2), P(1)–C(5) 1.807(2), C(1)–C(2) 1.511(2), C(2)–C(3) 1.381(3), C(3)–C(4) 1.489(3), C(4)–C(5) 1.413(2), C(3)–N(1) 1.357(2), C(1)–P(1)–C(5) 99.64(8), C(1)–P(1)–O(1) 120.41(11), O(1)–P(1)–P(1a) 118.44(10), C(5)–P(1)–P(1a) 103.33(6).

obtained for another 2-*t*Bu–3-OC(O)CHPh₂–3-Ph-1-phosphanaphthalene^[25] (1.746(5) and 1.720(4) Å) and are in the line with values found in aromatic phosphinines^[26] (~1.730–1.758 Å). The C1–P1–C5 bonding angle of 100.4(2)° is again similar to those established in the above mentioned analogues.^[25,26] The C–C bond lengths within the 1-phosphanaphthalene core are comparable with those of the parent naphthalene.^[27]

The ³¹P{¹H} NMR spectra of **4** and **5** contained signals at $\delta(^{31}\text{P}) = 168.3$ and 165.1 ppm, respectively, being well comparable to other 1-phosphanaphthalenes.^[25,28] The ¹H NMR spectra revealed the signals of the NHDipp at $\delta(^1\text{H}) = 9.22$ and 6.16 ppm, while the ¹H, ¹⁵N-HMBC spectra showed doublets at –297 and –300 ppm (¹J_{N,H} ~ 92–93 Hz) similar to the arsenic analogues.^[16] The IR and Raman spectra of **4** and **5** revealed

single band for N–H stretching at ~3293 and 3436 cm^{–1}, respectively.

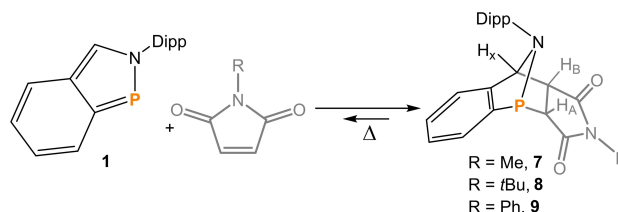
The molecular structure of **6** is shown in Figure 4. The hydrolysis resulted in the formation of a new P–P single bond (2.209(7), cf. $\Sigma_{\text{cov}}(\text{P}–\text{P}) = 2.22$ Å^[20]). The C=P bonds which were present in the original phospho-heterocycle became saturated to single-bonds (P1–C1, 1.837(2) Å). The oxygen atom is disordered over both P1(a) atoms (only one of them is shown in Figure 4) with the bond length 1.426(3) Å being shorter than $\Sigma_{\text{cov}}(\text{P}=\text{O}) = 1.59$ Å^[21]. Nevertheless, these data are comparable to similar compounds such as Ph₂P(O)PPh₂^[29] or R(Cy)P(O)PR(Cy)^[30] (R=(*t*Bu)C=CHPh).

The presence of two non-equivalent phosphorus atoms is reflected by the detection of two mutually coupled doublets at $\delta(^{31}\text{P}) = 32.3$ (PP=O) and –42.6 (PP=O) ppm with ¹J_{P,P} = 264 Hz falling among typical values found for similar P–P bonded species.^[29,30] The ¹H NMR spectra revealed two signals for the NHDipp at $\delta(^1\text{H}) = 11.45$ and 11.80 ppm, while the ¹H, ¹⁵N-HMBC spectra showed doublets for these groups at –279.9 and –279.2 ppm (¹J_{N,H} = 89 Hz). Two signals for the newly formed sp³ PC(H)(CO₂Me) groups were detected in the ¹H NMR spectrum at $\delta(^1\text{H}) = 4.63$ and 4.73 ppm and two signals were also observed for these groups in the ¹³C{¹H} NMR spectrum. The IR and Raman spectra of **6** showed a band due to the carbonyl function at 1735 cm^{–1} and the strong IR band at 1201 cm^{–1} was assigned to the P=O stretching mode.

To further prove the diene character of **1**, it was treated with *N*-alkyl/aryl-maleimides RN(C(O)CH)₂ (R=Me, *t*Bu, Ph) smoothly affording the addition products **7–9** (Scheme 4, Figure 5).

The molecular structures of **7** and **9** are closely related, the maleimides attacked the azaphosphole ring and two new covalent bonds P1–C3/20 (1.904(4) and 1.912(2) Å, for **7** and **9**, respectively), C4–C11 and C7–3 (1.562(5) and 1.581(1) Å) were formed. The bonding motif found in **7–9** resembles that obtained recently for the antimony analogue with one remarkable exception. In **7–9**, both CH groups of the maleimidic framework are oriented toward the bridgehead nitrogen atom (*endo*-form), while in the case of the antimony analogues^[31] *exo*-form is preferred.

The ³¹P{¹H} NMR spectra of **7–9** revealed one signal at $\delta(^{31}\text{P}) = 31.6$, 33.0 and 32.4 ppm, respectively. The ¹H NMR spectra showed a typical ABX pattern for two CH groups of the maleimidic framework and a C(H)NDipp group (Scheme 4). Similarly, the ¹³C{¹H} NMR spectra revealed three signals for this spin system. The IR and Raman spectra of **7–9** show a pair of



Scheme 4. Synthesis of **7–9** also showing the reversible binding of maleimides.

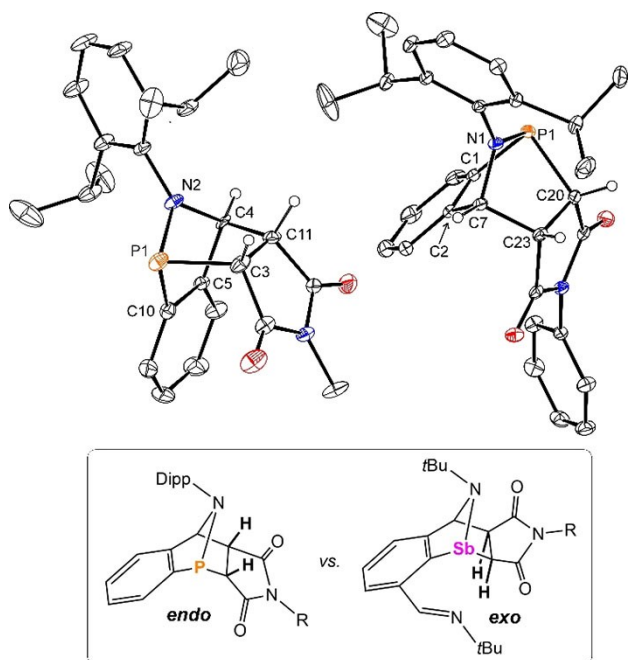


Figure 5. ORTEP presentation of the molecular structures of **7** (left) and **9** (right) (40% probability displacement ellipsoids). Hydrogen atoms except the relevant CH, and NH group are omitted. Bond lengths [Å] and angles [°]: Hydrogen atoms are omitted. Bond lengths [Å] and angles [°] for **7**: P(1)–N(2) 1.726(3), P(1)–C(3) 1.904(4), P(1)–C(10) 1.815(3), N(2)–C(4) 1.451(4), C(3)–C(11) 1.533(5), C(11)–C(4) 1.562(5), C(4)–C(5) 1.518(4), C(5)–C(10) 1.386(4), N(2)–P(1)–C(3) 86.85(14), N(2)–P(1)–C(10) 90.08(13), C(3)–P(1)–C(10) 91.94(15). **9**: P(1)–N(1) 1.703(2), P(1)–C(1) 1.842(2), P(1)–C(20) 1.912(2), N(1)–C(7) 1.470(2), C(20)–C(23) 1.535(2), C(23)–C(7) 1.581(1), C(7)–C(2) 1.515(2), C(2)–C(1) 1.400(2), N(1)–P(1)–C(1) 89.89(6), N(1)–P(1)–C(20) 88.37(6), C(1)–P(1)–C(20) 91.17(6). Inset shows a different type of maleimide bonding in antimony analogues.

bands at ~ 1766 and ~ 1697 cm^{-1} due to symmetric and antisymmetric C=O stretching mode being characteristic for cyclic imides.^[22]

Being aware of the reversibility of the maleimide-binding toward the antimony center in an *N,C,N*-chelated stibinidene 2,6-(*t*BuN=CH) $\text{C}_6\text{H}_3\text{Sb}$,^[31] a variable-temperature (VT) ^1H NMR study was undertaken. It turned out that upon warming of [D8] toluene solutions of **7–9**, the cycloadducts tend to decompose to the starting material **1** and the respective maleimides similarly to the antimony compounds. The calculated thermodynamic parameters, determined based on an experimental temperature dependence of equilibrium constant *K*, for reaction **1** + imide \rightarrow **7–9** at 298 K, point to a significant difference between the P and Sb systems (Table 2). It shows that the maleimide is significantly more tightly bonded to the phosphorus compound **1**. Based on these findings, it becomes obvious that the reversibility of the C=C bond activation in these maleimides is sensitive to the low-valent pnictogen system used.

Table 2. ΔG° [kcal mol $^{-1}$] and ΔH° [kcal mol $^{-1}$] values for reaction **1** + maleimide \rightarrow **7–9** at 298 K determined by a VT ^1H NMR study and their comparison with an analogous antimony system.

Compound	R ^[a]	ΔG°_{298}	ΔH°
1	Me	–7.26	–24.92
	<i>t</i> Bu	–10.97	–48.73
	Ph	–5.64	–17.66
2,6-(<i>t</i> BuN=CH) $\text{C}_6\text{H}_3\text{Sb}$ ^[b]	Me	–3.48	–16.51
	<i>t</i> Bu	–1.94	–16.39
	Ph	–2.59	–16.56

[a] Denotes the R substituent on the nitrogen in maleimides RN(C(O)CH) $_2$ (R=Me, *t*Bu, Ph). [b] from Ref. [31].

Reactivity of **1** as a hidden phosphinidene.

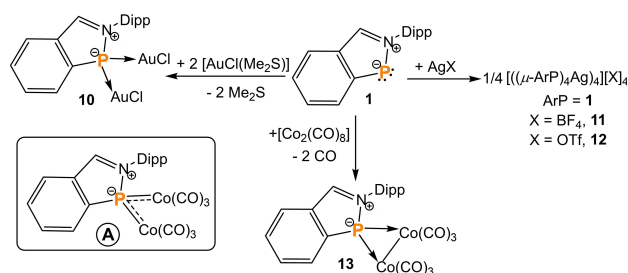
As we have demonstrated a heterodiene-like behavior of **1** above, we became curious if it may serve as a hidden phosphinidene as well and use its lone electron pairs for coordination of selected TMs (Scheme 5). Indeed, it turned out that **1** smoothly reacts with [AuCl(Me $_2$ S)] and AgX (where X=BF $_4$ or OTf) giving complexes $[\mu\text{-ArP}(\text{AuCl})_2]$ (**10**) and $[(\mu\text{-ArP})_4\text{Ag}_4][\text{X}]_4$ (X=BF $_4$ (**11**), OTf (**12**)). Similarly, the treatment of **1** with [Co $_2$ (CO) $_8$] produced the complex $[\mu\text{-ArP}(\text{Co}_2(\text{CO})_6)]$ (**13**).

In all cases, **1** plays a role of a bridging ligand, thereby sharing both lone pairs with the respective TMs. Such type of bonding has often been considered as a proof for phosphinidene character of the central phosphorus atom for example in (NHC)PR adducts or related complexes.^[10c,32]

The molecular structures of **10**, **12** and **13** were unambiguously established by single-crystal X-ray diffraction analysis and are shown in Figures 6–8.

In the structure of **10** (Figure 6), two independent molecules are connected via a weak aurophilic Au–Au contact (3.2613(6) Å). The central P atom is found in a tetrahedral coordination array and coordinates to two AuCl moieties with bond lengths in the range 2.215(3)–2.235(3) Å (cf. $\Sigma_{\text{cov}}(\text{P–Au}) = 2.35$ Å).^[20]

The Au–P distances are well comparable to complexes reported by Protasiewicz^[33] i.e. $[\mu\text{-Ar}'(\text{PMe}_3)\text{P}(\text{AuCl})_2]$ 2.236–2.247 Å (where Ar'=2,6-Mes $_2\text{C}_6\text{H}_3$ or Mes*), NHC-phosphinidene complexes such as $[\mu\text{-NHC}(\text{Ar}')\text{P}(\text{AuCl})_2]$ 2.232–2.252 Å (where Ar'=2,6-Mes $_2\text{C}_6\text{H}_3$ or Ph)^[32b,c,34] or peri-substitution stabilized phosphinidene gold complex 2.248–2.263 Å.^[35] The Au–P–Au bonding angles differ slightly being 114.26(10) and 118.73(10)



Scheme 5. Synthesis of complexes **10–13**.

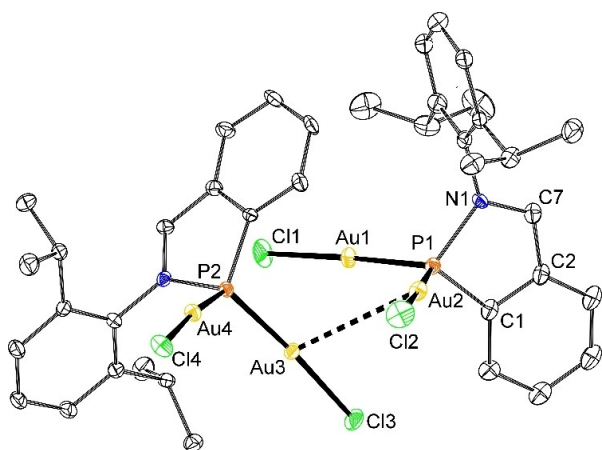


Figure 6. ORTEP presentation of the molecular structures of **10** showing (40% probability displacement ellipsoids). Hydrogen atoms and dichloromethane solvent molecules are omitted. Bond lengths [Å] and angles [°]: P(1)–N(1) 1.798(9), P(2)–N(2) 1.791(8), P(1)–Au(1) 2.228(2), P(1)–Au(2) 2.216(3), P(2)–Au(3) 2.235(3), P(2)–Au(4) 2.222(2), Au(1)–Au(2) 3.2613(6), Au(1)–P(1)–Au(2) 114.26(10), Au(3)–P(2)–Au(4) 118.73(10).

and are wider than those in $[\mu\text{-Ar}'(\text{PMe}_3)\text{P}(\text{AuCl})_2]^{[31]}$ (98.92–103.19°) or $[\mu\text{-NHC}(\text{Ar})\text{P}(\text{AuCl})_2]^{[32\text{b,c},34]}$ 104.39–108.81°, but are comparable to the peri-substituted phosphinidene gold complex 118.40°. [35]

Complex **12** forms a tetramer (Figure 7). The Ag–P bond lengths (2.432(3)–2.451(3) Å) are slightly longer than $\Sigma_{\text{cov}}(\text{P}–\text{Ag}) = 2.39 \text{ Å}^{[20]}$ and the values in related complexes $[\mu\text{-Ar}'(\text{PMe}_3)\text{P}(\text{AgOTf})_2]^{[33]}$ (2.309 and 2.282 Å) or $[\mu\text{-NHC}(\text{Ar})\text{P}(\text{AgCl})_2]_{\infty}^{[32\text{c}]}$ (2.3573–2.3884 Å). The Ag–P–Ag angles of 99.59(10) and 97.93(8)° are more acute than P–Ag–P ones (166.85(11)–172.89(7)°). Two of the OTf anions are found outside the coordination sphere of the metal centers, while the remaining two form weak contacts with the silver atoms (Ag–O ~ 2.61 Å, cf. $\Sigma_{\text{cov}}(\text{O}–\text{Ag}) = 1.91 \text{ Å}^{[20]}$, see Figures S47). Similar complexes bearing central Ag_4P_4 cores described in literature mostly contain a charged R_2P^- phosphanide group, but the key structural data are similar for example $[\text{Ag}_4(\text{P}(\text{NR}_2)\text{C}_6\text{F}_5)_4]^{[36]}$, $[\text{Ag}_4(\text{cyclo}-(\text{P}_4\text{tBu}_3)\text{PtBu}_4)]^{[37]}$ or $[\text{Ag}_4(\text{P}(\text{PtBu}_2)\text{SiMe}_3)_4]^{[38]}$. In the case of **13** (Figure 8), the phosphorus atom bridges the cobalt atoms with similar P–Co bond lengths 2.118(6) and 2.139(6) Å both being shorter than $\Sigma_{\text{cov}}(\text{P}–\text{Co}) = 2.22 \text{ Å}^{[20]}$. By contrast, the Co–Co distance of 2.629(4) Å is significantly elongated in comparison with the $\Sigma_{\text{cov}}(\text{Co}–\text{Co}) = 2.22 \text{ Å}$. The Co1–P1–Co2 bond angle 76.29(2)° is very narrow in comparison with **10–12**, but is comparable to $[(\mu\text{-Mes}^*\text{P})(\text{Co}_2(\text{CO})_6)]$ (cf. Co–P distances 2.047 Å, Co–P–Co angle 82.0°). [39] For $[(\mu\text{-Mes}^*\text{P})(\text{Co}_2(\text{CO})_6)]$, the authors postulated a partially multiple Co–P bonds and it is likely to consider a similar situation for **13** (see below).

Upon isolation, complex **10** was only sparingly soluble in common solvents. Nevertheless, the ^1H and $^{31}\text{P}\{^1\text{H}\}$ NMR spectra in $[\text{D}]\text{chloroform}$ could be obtained and revealed one signal at $\delta(^{31}\text{P}) = 140.1 \text{ ppm}$. By contrast, complexes **11** and **12** exhibit good solubility in $[\text{D}_3]\text{acetonitrile}$. The ^1H and $^{13}\text{C}\{^1\text{H}\}$ NMR spectra showed rather similar features suggesting that the role of the counter-anion (BF_4 or OTf) on the structure in solution is

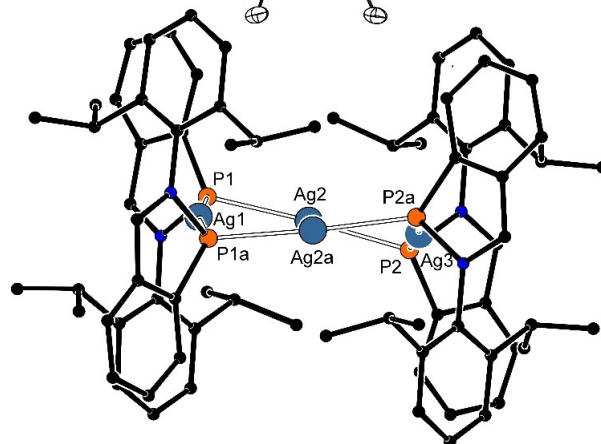
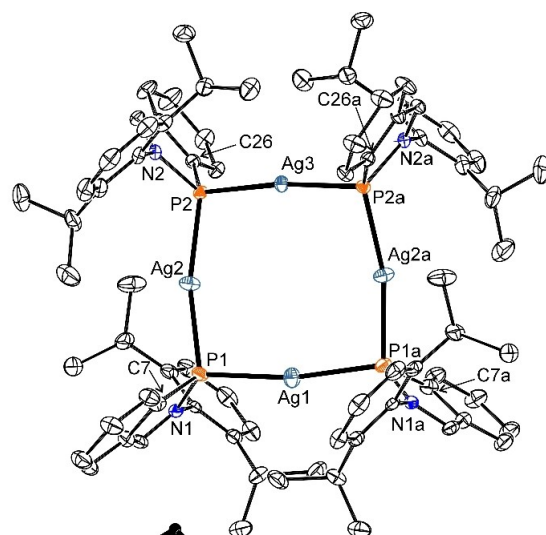


Figure 7. ORTEP presentation of the molecular structures of **12** (40% probability displacement ellipsoids). Hydrogen atoms, OTf anions and dichloromethane solvate molecules are omitted. Symmetry operator $a = 1 - x, y, 3/2 - z$. Bond lengths [Å] and angles [°]: Ag(1)–P(1) 2.451(3), Ag(2)–P(1) 2.439(2), Ag(2)–P(2) 2.445(2), Ag(3)–P(2) 2.432(3), P(1)–N(1) 1.752(7), P(2)–N(2) 1.752(7), P(1)–C(7) 1.775(11), P(2)–C(26) 1.772(8), Ag(1)–P(1)–Ag(2) 99.59(10), Ag(2)–P(2)–Ag(3) 97.93(8), P(1)–Ag(1)–P(1) 169.88(9), P(1)–Ag(2)–P(2) 166.85(11), P(2)–Ag(3)–P(2a) 172.89(7).

negligible. The $^{31}\text{P}\{^1\text{H}\}$ NMR spectra showed one signal at $\delta(^{31}\text{P}) = 150.8$ and 149.5 ppm, respectively. Furthermore, the measurement of high mass accuracy positive-ion electrospray full scan mass spectra (ESI-MS) of **12** in an acetonitrile solution revealed formation of a group of ions composed of one to four Ag atoms (see Supporting Information for details, Figure S57). All observed cluster ions are in accordance with the expected structure of the tetrameric complex and they are probably formed in the gas phase due to the consecutive fragmentation of the initial tetrameric complex. It indicates that the tetrameric structure is also retained in solution.

One set of sharp signals was also obtained for the ligand in the ^1H and $^{13}\text{C}\{^1\text{H}\}$ NMR spectra of **13**, the latter also contained signals for the carbonyl moieties at 206.3 ppm. Their presence was also corroborated by the infrared spectrum of solid **13** showing six strong absorption bands, while in the toluene solution only three carbonyl bands were observed at 2046,

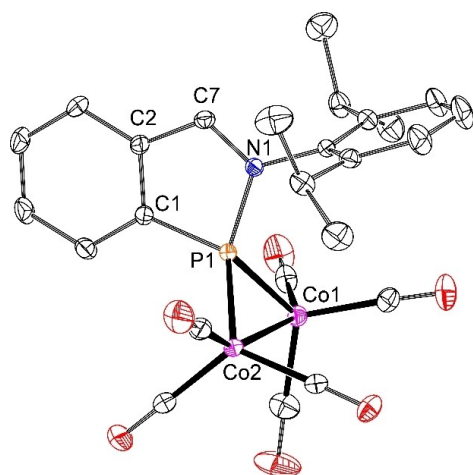


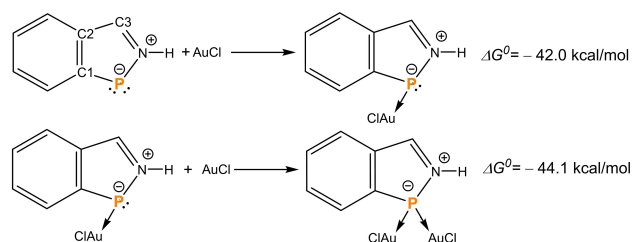
Figure 8. ORTEP presentation of the molecular structures of **13** (40% probability displacement ellipsoids). Hydrogen atoms are omitted. Bond lengths [Å] and angles [°]: P(1)–N(1) 1.795(2), P(1)–C(1) 1.788(2), P(1)–Co(1) 2.118(6), P(1)–Co(2) 2.139(6), Co(1)–Co(2) 2.629(4), Co(1)–P(1)–Co(2) 76.29(2), C(1)–P(1)–N(1) 88.10(9).

2005 and 1978 cm^{-1} see Figure S56. These values are shifted in comparison with those reported for a hexane solution of $[(\mu\text{-Mes}^*\text{P})(\text{Co}_2(\text{CO})_6)]$: 2070 and 2020 cm^{-1} .^[39] The $^{31}\text{P}\{\text{H}\}$ NMR spectrum contained one signal at 265.6 ppm that is significantly down field in comparison with **10–12**, however, the structural analogue $[(\mu\text{-Mes}^*\text{P})(\text{Co}_2(\text{CO})_6)]$ revealed an even more deshielded signal at 664 ppm being consistent with some multiple bonding between phosphorus and cobalt atoms (Scheme 5A).^[39]

We examined computationally in more detail the complex formation reaction leading to **10**. In comparison with the model

Table 3. Selected Wiberg Bond Indices (WBI), NPA-charges (q , [e^-]) and net charge transfer (Δq , [e^-]) for model compounds at the $\omega\text{B97XD}/\text{def2-TZVP}$ level.

WBI	1'	1'(AuCl)	1'(AuCl)₂	H₃P(AuCl)	1'(Co₂(CO)₆)
P–M		0.64	0.61	0.65	0.79/0.81
P–N	0.96	0.84	0.73		0.72
P–C1	1.29	1.12	0.96		0.96
N–C3	1.29	1.42	1.55		1.51
Co–Co					0.41
$q(\text{P})$	0.623	0.603	0.558	0.163	1.327
$q(\text{M})$		0.243	0.282	0.304	–1.629/ –1.662
Δq		0.317	0.550	0.272	1.163



Scheme 6. Computed model reactions at the $\omega\text{B97XD}/\text{def2-TZVP}$ level.

benzazaphosphole (**1'**), we investigated its mono- and di-complexation with AuCl leading to **1'(AuCl)**, and **1'(AuCl)₂**. As the number of the AuCl moieties grows, the P–N and the C1–P1 bonds weaken, however, the N–C3 bonds strengthen, and therefore the weight of the zwitterionic resonance structure **1'B** gets more pronounced in the complexes (Tables 1 and 3).

To understand the complex formation reaction, we investigated the energetic consequences of the stepwise complexation process (Scheme 6). As it can be seen from the complexation Gibbs free energies, the two lone pairs of the phosphorus center react very similarly (the Gibbs free energies in the consecutive complexation steps are nearly equal), highlighting the presence of resonance structure **1'B** in the description of ligand **1'**. This observation is further supported by the net charge transfer (Δq), calculated as the NPA charges transferred from the ligand **1'** to the AuCl moieties. The net charge transfer (Δq) grows similarly with the number of the AuCl moieties (in **1'(AuCl)** $\Delta q = 0.317 e^-$, in **1'(AuCl)₂** $\Delta q = 0.550 e^-$ and both exceed that of $0.272 e^-$ in $\text{H}_3\text{P} \rightarrow \text{AuCl}$). The WBIs of the P→Au interactions are also very similar in both AuCl complexes of **1'** and $\text{H}_3\text{P} \rightarrow \text{AuCl}$.

The structure and charge distribution of complex **13** were also investigated by DFT-calculations (on a model complex **13'**, in which the ligand **1** was replaced by the parent ligand **1'**). Compared to the complexes **1'(AuCl)** and **1'(AuCl)₂**, the net charge transfer in the cobalt complex is even more significant ($\Delta q = 1.163 e^-$), which is in good agreement with the unusually low-field ^{31}P NMR chemical shift observed for complex **13**, being indicative for possible multiple bonding (Scheme 5A). Furthermore, the WBI of the Co–P bond in **13'** also shows a rather strong interaction ($\text{WBI}(\text{P} \rightarrow \text{Co}) = 0.79/0.81$, in contrast to **1'(AuCl)₂** $\text{WBI}(\text{P} \rightarrow \text{Au}) = 0.61$. The atoms in molecules analysis on complex **13'** revealed bond critical points between the P and Co-centers, however, no bond critical points were found between the two Co-centers (Figure S58), which excludes the presence of significant metal-metal interactions in the complex.

Conclusion

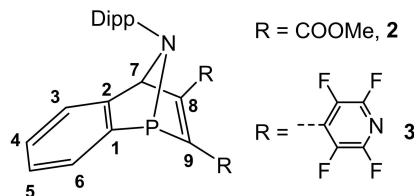
Based on a detailed theoretical study, we have predicted that the titled 2,1-benzazaphosphole **1** can exhibit a dual behavior and serve as a heterodiene or as a hidden phosphinidene. This presumption has been confirmed by chemical experiments. Thus, **1** reacts as a heterodiene in Diels-Alder type processes with activated carbon-carbon triple and double bonds forming expected bicyclic compounds. Furthermore, the spontaneous or pyridine promoted hydrogen migration in the structure of the products allowed the isolation of aromatic 1-phosphanaphthalenes. In contrast, compound **1** is able to play the role of a 4e ligand to metal centers such as Au, Ag or Co as well, which is considered to be an inherent property of phosphinidenes or phosphides. This remarkable ability to switch the reactivity of **1** will be further studied by our group as we will continue in seeking for related group 15 compounds.

Experimental Section

General remarks

All manipulations were carried out under inert atmosphere using standard Schlenk tube technique. Solvents were dried using the MD7 Pure Solv instrument (Innovative Technology, MA, USA). [D6] benzene, [D3]acetonitrile, [D]chloroform and [D2]dichloromethane were dried by standard procedure and stored over potassium mirror (benzene) or over molecular sieves (acetonitrile, chloroform and dichloromethane). The ^1H , $^{13}\text{C}\{^1\text{H}\}$, $^{19}\text{F}\{^1\text{H}\}$ and $^{31}\text{P}\{^1\text{H}\}$ NMR spectra were recorded on Bruker Ultrashield 400 or Bruker Ascend 500 spectrometer, using 5 mm tunable broad-band probe or cryoprobe Prodigy. Appropriate chemical shifts in ^1H and $^{13}\text{C}\{^1\text{H}\}$ NMR spectra were related to the residual signals of the solvents ([D6] benzene: $\delta(^1\text{H})=7.16$ ppm and $\delta(^{13}\text{C})=128.39$ ppm, [D3] acetonitrile: $\delta(^1\text{H})=1.94$ ppm and $\delta(^{13}\text{C})=1.39$ ppm, [D]chloroform: $\delta(^1\text{H})=7.27$ ppm and $\delta(^{13}\text{C})=77.23$ ppm, [D2]dichloromethane: $\delta(^1\text{H})=5.32$ ppm and $\delta(^{13}\text{C})=54.00$ ppm). The assignment of signals in NMR spectra was achieved using techniques such as ^{13}C -APT, ^1H , ^1H -COSY, ^1H , ^{13}C -HSQC, ^1H , ^{13}C -HMBC or ^1H , ^{15}N -HMBC experiments. Elemental analyses were performed on an LECO-CHNS-932 analyzer. IR spectra were recorded on a Nicolet iS50 FTIR spectrometer using a single-bounce silicon or diamond ATR crystals. Raman spectra were recorded in the range 4000–100 cm^{-1} with a Nicolet iS50 equipped with iS50 Raman module (excitation laser 1064 nm). Raman spectrum of **13** was not obtained due to sample decomposition on laser irradiation. Starting compounds **1** was synthesized according to the literature.^[12] Bis(tetrafluoropyridyl)ethyne was synthesized by a modified procedure described elsewhere.^[40] All other starting compounds were obtained from commercial sources and used as delivered.

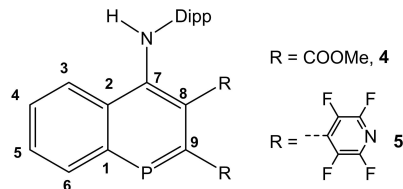
Synthesis of 2 and 3



2: 246 mg of **1** (0.83 mmol) was suspended in 20 mL of hexane. While stirring at -20°C , 292 μL (0.83 mmol) of dimethylacetylene dicarboxylate (DMAD) was added dropwise. After stirring for 10 min at -20°C , the resulting yellow mixture was filtered. The yellow filtrate was concentrated to ca. 5 mL and left to crystallize at -30°C yielding of light-yellow polycrystalline **2**. Yield 286 mg (78%), M.p. 79°C . Anal. Calcd. for $\text{C}_{25}\text{H}_{28}\text{NO}_4\text{P}$: C, 68.6; H, 6.5; N, 3.2; O, 14.6. Found: C, 68.8; H, 6.6; N, 3.1; O 14.6. ^1H NMR (500 MHz, C_6D_6): δ 0.89 (s, 6H, $\text{CH}(\text{CH}_3)_2$), 1.32 (s, 6H, $\text{CH}(\text{CH}_3)_2$), 2.73 (s, 1H, $\text{CH}(\text{CH}_3)_2$), 3.26 (s, 3H, COOCH_3), 3.36 (s, 3H, COOCH_3), 3.50 (s, 1H, $\text{CH}(\text{CH}_3)_2$), 5.64 (d, $^1J_{\text{P,H}}=2.3$ Hz, 1H, H7), 6.72 (m, 1H, H5), 6.79 (dd, 1H, H4), 7.02 (br., 1H, Dipp-H), 7.10 (br., 2H, Dipp-H), 7.34 (d, $^3J_{\text{P,C}}=7.1$ Hz, 1H, H3), 7.52 (dd, 1H, H6) ppm. $^{13}\text{C}\{^1\text{H}\}$ NMR (126 MHz, C_6D_6): δ 24.2 (s, $\text{CH}(\text{CH}_3)_2$), 24.7 (s, $\text{CH}(\text{CH}_3)_2$), 30.1 (s, $\text{CH}(\text{CH}_3)_2$), 31.0 (s, $\text{CH}(\text{CH}_3)_2$), 52.1 (s, COOCH_3), 52.2 (s, COOCH_3), 82.4 (d, $^3J_{\text{P,C}}=8.0$ Hz, C7), 123.1 (s, C3), 124.5 (br., Dip-C), 124.5 (br., Dip-C), 125.6 (d, $^3J_{\text{P,C}}=8.0$ Hz, C5), 127.6 (s, C4), 127.9 (s, Dip-C), 128.7 (d, $^2J_{\text{P,C}}=24.3$ Hz, C6), 141.7 (d, $^2J_{\text{P,C}}=11.8$ Hz, Dip-C), 148.2 (s, Dip-C), 149.1 (s, Dip-C), 151.5 (d, $^1J_{\text{P,C}}=19.0$ Hz, C1), 152.0 (s, C2), 157.2 (s, C8), 161.7 (d, $^1J_{\text{P,C}}=35.2$ Hz, C9), 164.1 (d, $^3J_{\text{P,C}}=1.7$ Hz, CO), 166.9 (d, $^2J_{\text{P,C}}=19.7$ Hz, CO) ppm. $^{31}\text{P}\{^1\text{H}\}$ NMR (202 MHz, C_6D_6): δ 39.9 (s) ppm. IR [cm^{-1}]: 1726 s, 1707 s ($\nu_{\text{C=O}}$). Raman [cm^{-1}]: 1729 m, 1707 m ($\nu_{\text{C=O}}$), 1610 m ($\nu_{\text{C=C}}$).

3: 233 mg of **1** (0.79 mmol) and 255 mg (0.79 mmol) of bis(perfluoro-4-pyridyl)ethyne were dissolved in 10 mL of toluene at ambient temperature. The reaction mixture was stirred for 2 h at 100°C . Subsequently, the yellow mixture was evaporated and extracted with hexane at 60°C . The extract was crystallized at ambient temperature giving yellow crystals of **3**. The single crystals grown from hexane contained one molecule of the starting alkyne in the unit cell. It is to note, that traces of this alkyne in the bulk sample of **3** were also detected by $^{19}\text{F}\{^1\text{H}\}$ NMR spectroscopy and could not be removed even by repeated crystallization. Nevertheless, the purity was shown to be sufficient for subsequent reaction. Yield 204 mg (42%), M.p. 159°C . ^1H NMR (500 MHz, C_6D_6): δ 0.91 (d, $^3J=6.8$ Hz, 3H, $\text{CH}(\text{CH}_3)_2$), 0.96 (d, $^3J=6.8$ Hz, 3H, $\text{CH}(\text{CH}_3)_2$), 1.23 (d, $^3J=6.8$ Hz, 6H, $\text{CH}(\text{CH}_3)_2$), 2.59 (sept, $^3J=6.8$ Hz, 1H, $\text{CH}(\text{CH}_3)_2$), 3.43 (sept, $^3J=6.8$ Hz, 1H, $\text{CH}(\text{CH}_3)_2$), 5.26 (s, 1H, H7), 6.80 (m, 2H, H4 + H5), 7.04 (d, 1H, Dipp-H), 7.07 (s, 1H, H3), 7.13 (m, 2H, Dipp-H), 7.58 (m, 1H, H6) ppm. $^{13}\text{C}\{^1\text{H}\}$ NMR (126 MHz, C_6D_6): δ 23.4 (s, $\text{CH}(\text{CH}_3)_2$), 24.1 (s, $\text{CH}(\text{CH}_3)_2$), 25.0 (s, $\text{CH}(\text{CH}_3)_2$), 25.6 (s, $\text{CH}(\text{CH}_3)_2$), 30.2 (s, $\text{CH}(\text{CH}_3)_2$), 30.9 (s, $\text{CH}(\text{CH}_3)_2$), 84.4 (d, $^3J_{\text{P,C}}=7.9$ Hz, C7), 123.1 (s, C3), 124.6 (s, Dip-C), 124.7 (s, Dip-C), 126.1 (d, $^3J_{\text{P,C}}=8.0$ Hz, C5), 127.8 (s, C4), 128.6 (s, Dip-C), 128.9 (d, $^2J_{\text{P,C}}=25.1$ Hz, C6), 129.6 (m, $\text{C}_6\text{F}_4\text{N-C}$), 137.4 (m, $\text{C}_6\text{F}_4\text{N-C}$), 139.5 (m, $\text{C}_6\text{F}_4\text{N-C}$), 141.1 (m, $\text{C}_6\text{F}_4\text{N-C}$), 141.2 (d, $^3J_{\text{P,C}}=12.6$ Hz, Dip-C), 142.7 (m, $\text{C}_6\text{F}_4\text{N-C}$), 143.2 (m, $\text{C}_6\text{F}_4\text{N-C}$), 144.6 (m, $\text{C}_6\text{F}_4\text{N-C}$), 145.2 (m, $\text{C}_6\text{F}_4\text{N-C}$), 148.6 (s, Dip-C), 149.7 (s, Dip-C), 151.0 (s, C2), 151.1 (d, $^1J_{\text{P,C}}=19.1$ Hz, C1), 154.5 (s, C8), 155.2 (d, $^1J_{\text{P,C}}=32.1$ Hz, C9) ppm. $^{19}\text{F}\{^1\text{H}\}$ (376 MHz, C_6D_6): δ -140.8 (m), -139.6 (m), -89.4 (m), -88.8 (m) + minor signals for bis(perfluoro-4-pyridyl)ethyne -136.5 and -89.4 ppm. $^{31}\text{P}\{^1\text{H}\}$ NMR (162 MHz, C_6D_6): δ 40.7 (t, $^3J_{\text{P,F}}=33.9$ Hz) ppm. IR [cm^{-1}]: 1645 m, 1461 vs. ($\nu_{\text{C=C}} + \nu_{\text{C-F}}$, tetrafluoropyridyl ring), 1615 w-sh ($\nu_{\text{C=C}}$). Raman [cm^{-1}]: 2250 vs. ($\nu_{\text{C=C}}$, bis(tetrafluoropyridyl)ethyne), 1646 vs., 1466 m ($\nu_{\text{C=C}} + \nu_{\text{C-F}}$, tetrafluoropyridyl ring), 1614 m ($\nu_{\text{C=C}}$).

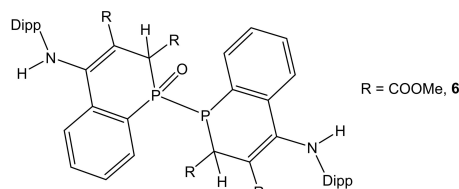
Synthesis of 4 and 5



4: 286 mg (0.65 mmol) of **3** was dissolved in 5 mL of pyridine and left stirring in a Young-valve sealed tube at 55°C for 1 h. The slightly darker solution was then evaporated to give an oil, which was extracted with hexane, concentrated and crystallized at -30°C to give 0.194 g of precipitate characterized as **4**. Yield 194 mg (68%), M.p. 139°C . Anal. Calcd. for $\text{C}_{25}\text{H}_{28}\text{NO}_4\text{P}$: C, 68.6; H, 6.5; N, 3.2; O, 14.6. Found: C, 68.9; H, 6.7; N, 3.3; O 14.8. ^1H NMR (500 MHz, C_6D_6): δ 0.79 (d, $^3J=6.8$ Hz, 6H, $\text{CH}(\text{CH}_3)_2$), 1.04 (d, 6H, $^3J=6.85$ Hz, $\text{CH}(\text{CH}_3)_2$), 3.11 (sept, $^3J=6.80$ Hz, 2H, $\text{CH}(\text{CH}_3)_2$), 3.55 (s, 3H, COOCH_3), 3.58 (s, 3H, COOCH_3), 6.78 (dd, 1H, H5), 6.86 (dd, 1H, H4), 7.04 (d, $^3J=7.5$ Hz, 2H, Dip-H), 7.11 (t, $^3J=7.0$ Hz, 1H, Dip-H), 7.85 (d, $^3J=8.7$ Hz, 1H, H3), 8.02 (dd, 1H, H6), 9.21 (s, 1H, NH) ppm. $^{13}\text{C}\{^1\text{H}\}$ NMR (126 MHz, C_6D_6): δ 22.4 (s, $\text{CH}(\text{CH}_3)_2$), 24.8 (s, $\text{CH}(\text{CH}_3)_2$), 29.2 (s, $\text{CH}(\text{CH}_3)_2$), 52.8 (s, COOCH_3), 52.9 (s, COOCH_3), 119.7 (d, $^2J_{\text{P,C}}=15.1$ Hz, C8), 124.9 (s, Dip-C), 127.2 (s, Dip-C), 127.2 (s, C4), 128.5 (s, C3), 129.1 (d, $^3J_{\text{P,C}}=4.3$ Hz, C5), 130.4 (d, $^2J_{\text{P,C}}=44.7$ Hz, C2), 136.4 (d, $^2J_{\text{P,C}}=42.0$ Hz, C6), 139.0 (s, Dip-C), 144.2 (s, Dip-C), 148.7 (d, $^3J_{\text{P,C}}=10.8$ Hz, C7), 152.1 (d, $^1J_{\text{P,C}}=9.3$ Hz, C1), 164.2 (d, $^1J_{\text{P,C}}=44.4$ Hz, C9), 170.1 (d, $^2J_{\text{P,C}}=23.7$ Hz, CO), 171.0 (s, CO) ppm. $^{31}\text{P}\{^1\text{H}\}$ NMR (202 MHz, C_6D_6): δ 168.3 (s) ppm. ^{15}N NMR (2D-HMBC, 51 MHz, C_6D_6): δ -297 (d, $^1J_{\text{N,H}}=92$ Hz, NH) ppm. IR [cm^{-1}]: 3288 m-br ($\nu_{\text{N-H}}$), 1713 s, 1684 s ($\nu_{\text{C=O}}$). Raman [cm^{-1}]: 3298 w-br ($\nu_{\text{N-H}}$), 1714 m, 1686 m ($\nu_{\text{C=O}}$).

5: 204 mg (0.33 mmol) of **3** was dissolved in 10 mL of toluene and stirred at 120 °C for 24 h. Then, the dark-yellow solution was evaporated, washed with hexanes and then re-dissolved in 5 mL of toluene and crystallized at 0 °C to give orange single crystals of **5**. Yield 148 mg (71%), M.p. 217 °C. Anal. Calcd. for C₃₁H₂₇F₈N₃P: C, 60.1; H, 3.6; N, 6.8. Found: C, 60.0; H, 3.5; N, 7.1. ¹H NMR (500 MHz, C₆D₆): δ 0.74 (d, ³J=6.7 Hz, 6H, CH(CH₃)₂), 0.99 (d, ³J=6.7 Hz, 6H, CH(CH₃)₂), 2.82 (sept, ³J=6.7 Hz, 6H, CH(CH₃)₂), 6.16 (s, 1H, NH), 6.78 (d, ³J=7.7 Hz, 2H, Dip-H), 6.86 (d, ³J=7.6 Hz, 1H, Dip-H), 7.13 (dd, 1H, H5), 7.23 (dd, 1H, H4), 8.07 (m, 2H, H3,6) ppm. ¹³C{¹H} NMR (126 MHz, C₆D₆): δ 21.1 (s, CH(CH₃)₂), 25.5 (s, CH(CH₃)₂), 29.0 (s, CH(CH₃)₂), 115.0 (d, ²J_{P,C}=14.4 Hz, C8), 124.1 (s, Dip-C), 124.3 (s, C3), 127.4 (s, Dip-C), 127.6 (d, ³J_{P,C}=20.2 Hz, C5), 130.4 (d, ²J_{P,C}=10.4 Hz, C2), 130.9 (d, ⁴J_{P,C}=4.2 Hz, C4), 131.9 (m, C₆F₄N-C), 134.5 (m, C₆F₄N-C), 136.1 (d, ¹J_{P,C}=42.2 Hz, C6), 136.9 (s, Dip-C), 138.7 (m, C₆F₄N-CF), 140.8 (m, C₆F₄N-CF), 142.9 (m, C₆F₄N-CF), 143.9 (s, Dip-C), 144.9 (m, C₆F₄N-CF) 146.3 (d, ³J_{P,C}=12.9 Hz, C7), 152.3 (d, ¹J_{P,C}=46.6 Hz, C1), 156.8 (d, ¹J_{P,C}=42.4 Hz, C9) ppm. ¹⁹F{¹H} NMR (376 MHz, C₆D₆): δ -141.1 (m), -137.5 (m), -89.8 (m) ppm. ³¹P{¹H} NMR (202 MHz, C₆D₆): δ 165.1 (s) ppm. ¹⁵N NMR (2D-HMBC, C₆D₆): δ -300 (d, ¹J_{N,H}=91 Hz, NH) ppm. IR [cm⁻¹]: 3436 m (ν_{N-H}), 1640s, 1464vs. (ν_{C=C}+ν_{C-F}, tetrafluoropyridyl ring). Raman [cm⁻¹]: 3436 m (ν_{N-H}), 1645 m, 1468 m-sh (ν_{C=C}+ν_{C-F}, tetrafluoropyridyl ring).

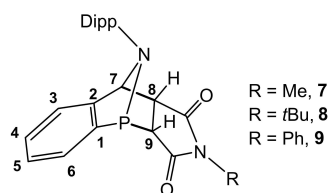
Preparation of single-crystals of **6**



Crude compound **4** was dissolved in a benzene-hexane mixture and left for crystallization for several weeks at -30 °C. During that time colorless single-crystals of **6** formed that were characterized by X-ray diffraction technique and subsequently by NMR, IR and Raman spectroscopy see below. M.p. 259 °C. ¹H NMR (500 MHz, CDCl₃): δ 0.40 (d, ³J=6.7 Hz, 3H, CH(CH₃)₂), 0.51 (d, ³J=6.7 Hz, 3H, CH(CH₃)₂), 1.04 (d, ³J=6.7 Hz, 3H, CH(CH₃)₂), 0.51 (d, ³J=6.7 Hz, 3H, CH(CH₃)₂), 1.38 (m, 6H, CH(CH₃)₂), 1.42 (m, 6H, CH(CH₃)₂), 3.08 (m, 1H, CH(CH₃)₂), 3.15 (sept, ³J=6.7 Hz, 1H, CH(CH₃)₂), 3.52 (m, 1H, CH(CH₃)₂), 3.53 (s, 3H, COOCH₃), 3.54 (s, 3H, COOCH₃), 3.60 (sept, ³J=6.7 Hz, 1H, CH(CH₃)₂), 3.74 (s, 3H, COOCH₃), 3.90 (s, 3H, COOCH₃), 4.63 (d, ²J_{P,C}=22.2 Hz, 1H, PC(H)(CO₂Me)), 4.73 (m, 1H, PC(H)(CO₂Me)), 6.92 (m, 1H, Ar-H), 7.01 (m, 2H, Ar-H), 7.05 (t, ⁿJ=4.5 Hz, 2H, Ar-H), 7.19 (m, 2H, Ar-H), 7.26 (m, 2H, Ar-H), 7.29 (m, 2H, Ar-H), 7.48 (m, 2H, Ar-H), 8.01 (m, 2H, Ar-H), 11.45 (s, 1H, NH), 11.80 (s, 1H, NH) ppm. ¹³C{¹H} NMR (126 MHz, C₆D₆): δ 20.7 (s, CH(CH₃)₂), 20.8 (s, CH(CH₃)₂), 22.8 (s, CH(CH₃)₂), 22.9 (s, CH(CH₃)₂), 24.6 (s, CH(CH₃)₂), 24.7 (s, CH(CH₃)₂), 24.9 (s, CH(CH₃)₂), 25.7 (s, CH(CH₃)₂), 28.3 (s, CH(CH₃)₂), 28.4 (s, CH(CH₃)₂), 29.4 (s, CH(CH₃)₂), 29.4 (s, CH(CH₃)₂), 34.9 (d, ¹J_{P,C}=17.0 Hz, PC(H)), 42.6 ppm (dd, ¹J_{P,C}=45.3 Hz and ²J_{P,C}=6.2 Hz, PC(H)), 51.6 (s, COOCH₃), 51.8 (s, COOCH₃), 52.5 (s, COOCH₃), 52.9 (s, COOCH₃), 123.5 (s, Ar-CH), 123.9 (s, Ar-CH), 124.4 (s, Ar-CH), 124.7 (s, Ar-CH), 126.4 (d, Ar-C), 126.6 (d, Ar-C), 127.1 (s, Ar-CH), 127.9 (s, Ar-CH), 127.8 (s, Ar-C), 128.1 (d, Ar-C), 128.6 (d, Ar-CH), 128.9 (d, Ar-CH), 129.2 (s, Ar-CH), 130.0 (s, Ar-CH), 130.1 (d, Ar-C), 130.7 (d, Ar-CH), 130.7 (d, Ar-C), 131.5 (s, Ar-CH), 132.5 (d, Ar-CH), 133.7 (d, Ar-C), 134.8 (m, Ar-C), 135.0 (s, Ar-C), 136.0 (s, Ar-C), 137.6 (dd, Ar-CH), 144.5 (s, Ar-C), 144.5 (s, Ar-C), 144.6 (s, Ar-C), 145.7 (s, Ar-C), 155.8 (s, Ar-C), 156.7 (d, Ar-C), 168.7 (d, ²J_{P,C}=3.7 Hz, CO), 169.9 (s, CO), 170.3 (d, ²J_{P,C}=7.5 Hz, CO), 172.4 (m, CO) ppm. ¹⁵N NMR (2D-HMBC, CDCl₃): δ -279.9 (d, ¹J_{N,H}=89 Hz, NH), -279.2 (d, ¹J_{N,H}=89 Hz, NH) ppm. ³¹P{¹H} NMR (162 MHz, C₆D₆): δ 32.3 (d,

¹J_{P,P}=264.0 Hz) and -42.6 (d, ¹J_{P,P}=264.0 Hz) ppm. IR [cm⁻¹]: 3165vw-br (ν_{N-H}), 1735 s, 1715 m-sh (ν_{C=O}), 1201vs. (ν_{P=O}). Raman [cm⁻¹]: 3167w,1736w (ν_{C=O}).

Synthesis of 7–9



7: 320 mg of **1** (1.08 mmol) was dissolved in 5 mL of hexane. The solution was added to 120 mg (1.08 mmol) of N-methylmaleimide dissolved in hexane. After stirring for 30 min. a tiny amount of a white precipitate formed. The reaction mixture was concentrated, filtered, and crystallized at ambient temperature, giving single crystals of **7**. Yield 416 mg (94%), M.p. 164–172 °C. Anal. Calcd. for C₂₄H₂₇N₂O₂P: C, 70.9; H, 6.7; N, 6.9. Found: C, 70.8; H, 6.8; N, 8.0. ¹H NMR (500 MHz, C₆D₆): δ 0.76 (s, 6H, CH(CH₃)₂), 1.17 (s, 6H, CH(CH₃)₂), 2.08 (s, 3H, NCH₃), 2.39 (br., 1H, CH(CH₃)₂), 2.88 (br., 1H, CH(CH₃)₂), 3.14 (m, 1H, H8), 3.50 (m, 1H, H9), 4.84 (m, 1H, H7), 6.82 (m, 1H, H5), 6.87 (dd, 1H, H4), 6.94 (br., 1H, Dip-H), 7.03 (br., 1H, Dip-H), 7.08 (t, ³J=7.0 Hz, 1H, Dip-H), 7.14 (d, ³J=7.1 Hz, 1H, H3), 7.33 (m, 1H, H6) ppm. ¹³C{¹H} NMR (126 MHz, C₆D₆): δ 23.9 (s, NCH₃), 24.1 (s, CH(CH₃)₂), 24.6 (s, CH(CH₃)₂), 24.8 (s, CH(CH₃)₂), 25.3 (s, CH(CH₃)₂), 29.7 (s, CH(CH₃)₂), 29.8 (s, CH(CH₃)₂), 48.4 (s, C8), 50.9 (d, ¹J_{P,C}=20.9 Hz, C9), 76.4 (d, ²J_{P,C}=7.1 Hz, C7), 122.2 (s, C3), 124.2 (s, Dip-C), 124.7 (s, Dip-C), 127.5 (d, ²J_{P,C}=22.6 Hz, C6), 127.6 (s, Dip-C), 127.7 (d, ³J_{P,C}=6.9 Hz, C5), 128.8 (s, C4), 140.7 (d, ²J_{P,C}=11.9 Hz, Dip-C), 144.2 (d, ¹J_{P,C}=20.0 Hz, C1), 148.0 (br, Dip-C), 148.0 (s, C2), 149.2 (br., Dip-C), 174.1 (s, CO), 174.7 (s, CO) ppm. ³¹P{¹H} NMR (202 MHz, C₆D₆): δ 31.6 (s) ppm. IR [cm⁻¹]: 1766 m (sym ν_{C=O}), 1693vs. (asym ν_{C=O}). Raman [cm⁻¹]: 1762 m (sym ν_{C=O}).

8: The procedure was analogous to that described above for **7**. 115 mg (0.39 mmol) of **1** and 56 μL (0.39 mmol) of N-t-butylmaleimide after workup gave **8** as a white powder. Yield 153 mg (88%), M.p. 169–173 °C. Anal. Calcd. for C₂₇H₃₃N₂O₂P: C, 72.3; H, 7.4; N, 6.3. Found: C, 72.6; H, 7.3; N, 6.5. ¹H NMR (500 MHz, C₆D₆): δ 0.72 (br., 6H, CH(CH₃)₂), 1.16 (br., 6H, CH(CH₃)₂), 1.18 (s, 9H, NC(CH₃)₃), 2.29 (br., 1H, CH(CH₃)₂), 2.87 (br., 1H, CH(CH₃)₂), 3.13 (m, 1H, H8), 3.51 (m, 1H, H9), 4.83 (m, 1H, H7), 6.82 (m, 1H, H5), 6.87 (dd, 1H, H4), 6.93 (br., 1H, Dip-H), 7.02 (br., 1H, Dip-H), 7.07 (t, ³J=7.6 Hz, 1H, Dip-H), 7.14 (d, ³J=7.3 Hz, 1H, H3), 7.33 (m, 1H, H6) ppm. ¹³C{¹H} NMR (126 MHz, C₆D₆): δ 24.1 (s, CH(CH₃)₂), 24.5 (s, CH(CH₃)₂), 24.8 (s, NCH(CH₃)₃), 25.4 (s, CH(CH₃)₂), 28.4 (s, NC(CH₃)₃), 29.7 (s, CH(CH₃)₂), 30.0 (s, CH(CH₃)₂), 47.5 (s, C8), 50.2 (d, ¹J_{P,C}=20.1 Hz, C9), 58.0 (s, C(CH₃)₃), 76.8 (d, ²J_{P,C}=7.1 Hz, C7), 122.6 (d, ³J_{P,C}=1.4 Hz, C3), 124.2 (s, Dip-C), 124.7 (s, Dip-C), 127.6 (d, ³J_{P,C}=7.2 Hz, C5), 127.6 (s, Dip-C4), 127.9 (d, ²J_{P,C}=22.4 Hz, C6), 128.9 (s, C4), 140.8 (d, ²J_{P,C}=11.8 Hz, Dip-C), 145.1 (d, ¹J_{P,C}=20.7 Hz, C1), 148.0 (br., Dip-C), 149.0 (s, C2), 149.2 (br., Dip-C), 175.3 (s, CO), 175.8 (s, CO). ³¹P{¹H} NMR (202 MHz, C₆D₆): δ 33.0 (s) ppm. IR [cm⁻¹]: 1761 m (sym ν_{C=O}), 1689vs. (asym ν_{C=O}). Raman [cm⁻¹]: 1762 m (sym ν_{C=O}), 1699w (asym ν_{C=O}).

9: The procedure was analogous to that described above for **7**. 115 mg (0.39 mmol) of **1** and 67 mg (0.39 mmol) of N-phenylmaleimide after workup gave **9** as colorless single-crystals. Yield 138 mg (76%), M.p. 217–221 °C. Anal. Calcd. for C₂₉H₂₉N₂O₂P: C, 74.3; H, 6.2; N, 6.0. Found: C, 74.4; H, 6.5; N, 5.7. ¹H NMR (500 MHz, C₆D₆): δ 0.73 (br., 3H, CH(CH₃)₂), 0.77 (br., 3H, CH(CH₃)₂), 1.21 (br., 6H, CH(CH₃)₂), 2.34 (br., 1H, CH(CH₃)₂), 2.90 (br., 1H, CH(CH₃)₂), 3.27 (m, 1H, H8), 3.62 (m, 1H, H9), 4.88 (m, 1H, H7), 6.79 (m, 4H, NPh-H), 6.93 (m, 2H, H4 + Dip-H), 7.1 (m, 5H, H3 + Dip-H + NPh-H), 7.34 (m, 1H,

H6) ppm. $^{13}\text{C}\{^1\text{H}\}$ NMR (126 MHz, C_6D_6): δ 24.1 (s, $\text{CH}(\text{CH}_3)_2$), 24.6 (s, $\text{CH}(\text{CH}_3)_2$), 24.8 (s, $\text{CH}(\text{CH}_3)_2$), 25.4 (s, $\text{CH}(\text{CH}_3)_2$), 29.8 (s, $\text{CH}(\text{CH}_3)_2$), 30.1 (s, $\text{CH}(\text{CH}_3)_2$), 48.2 (s, C8), 50.7 (d, $^1J_{\text{P,C}}=20.2$ Hz, C9), 76.7 (d, $^2J_{\text{P,C}}=6.9$ Hz, C7), 122.5 (s, C3), 124.2 (s, Dip-C), 124.7 (s, Dip-C), 126.9 (s, NPh-C), 127.7 (s, Dip-C), 127.8 (d, $^3J_{\text{P,C}}=19.2$ Hz, C6), 127.9 (s, C5), 128.5 (s, C4), 129.0 (s, NPh-C), 129.2 (s, NPh-C), 132.7 (s, NPh-C), 140.7 (d, $^2J_{\text{P,C}}=12.0$ Hz, Dip-C), 144.6 (d, $^1J_{\text{P,C}}=20.2$ Hz, C1), 148.0 (br., Dip-C), 148.3 (s, C2), 149.3 (br., Dip-C), 173.0 (s, CO), 173.6 (s, CO) ppm. $^{31}\text{P}\{^1\text{H}\}$ NMR (202 MHz, C_6D_6): δ 32.4 (s) ppm. IR [cm^{-1}]: 1770 m (sym $\nu_{\text{C=O}}$), 1708vs. (asym $\nu_{\text{C=O}}$). Raman [cm^{-1}]: 1770 m (sym $\nu_{\text{C=O}}$).

Synthesis of 10–13

10: 87 mg (0.29 mmol) of **1** was dissolved in 5 mL of dichloromethane and added to 171 mg (0.58 mmol) of $[\text{AuCl}(\text{Me}_2\text{S})]$ in 10 mL of acetonitrile and the reaction mixture clarified and turned intense yellow. After 5 min. of stirring at r.t. a precipitate started to form and the reaction mixture was stirred for additional 15 min. The precipitate was collected by filtration, dried in vacuo and characterized as **10**. The storage of the mother liquor provided second crop of single-crystals of **10**. Combined yield 165 mg (75%), M.p. 162 °C(dec.). Anal. Calcd. for $\text{C}_{20}\text{H}_{23}\text{Au}_2\text{Cl}_2\text{NP}$: C, 30.0; H, 2.9; N, 1.8. Found: C, 29.8; H, 2.8; N, 2.1. ^1H (400 MHz, CDCl_3): δ 1.14 (d, $^3J=6.8$ Hz, 3H, $\text{CH}(\text{CH}_3)_2$), 1.46 (d, $^3J=6.80$ Hz, 3H, $\text{CH}(\text{CH}_3)_2$), 3.19 (sept, $^3J=6.8$ Hz, 2H, $\text{CH}(\text{CH}_3)_2$), 7.39 (d, $^3J=7.9$ Hz, 2H, Dip-H), 7.62 (t, $^3J=7.9$ Hz, 1H, Dip-H), 7.86 (t, $^3J=7.2$ Hz, 1H, H5), 8.08 (m, 1H, H6), 8.32 (m, 2H, H3+H4), 8.78 (d, $^4J_{\text{P,H}}=11.70$ Hz, H7) ppm. $^{31}\text{P}\{^1\text{H}\}$ NMR (202 MHz, CDCl_3): δ 140.1 ppm.

11: 130 mg (0.44 mmol) of **1** dissolved in 5 mL of Et_2O was added to 86 mg (0.44 mmol) of AgBF_4 in 5 mL of Et_2O . A yellowish precipitate formed immediately and the reaction mixture was stirred for additional 15 min. The solid was collected by filtration, washed with 3 mL of Et_2O and 5 mL of hexane and dried in vacuo to give **11** as yellow powder. Yield 177 mg (82%), M.p. 111 °C(dec.). Anal. Calcd. for $\text{C}_{19}\text{H}_{22}\text{AgBF}_4\text{NP}$: C, 46.6; H, 4.5; N, 2.9. Found: C, 46.8; H, 4.6; N, 2.7. ^1H NMR (500 MHz, CD_3CN): δ 1.10 (d, $^3J=6.7$ Hz, 6H, $\text{CH}(\text{CH}_3)_2$), 1.18 (d, $^3J=6.7$ Hz, 6H, $\text{CH}(\text{CH}_3)_2$), 2.28 (sept, $^3J=6.7$ Hz, 2H, $\text{CH}(\text{CH}_3)_2$), 7.39 (m, 4H, H4+H5+Dip-H), 7.53 (t, $^3J=7.8$ Hz, 1H, Dip-H), 8.01 (m, 1H, H3), 8.16 (m, 1H, H6), 8.47 (s, 1H, H7) ppm. $^{13}\text{C}\{^1\text{H}\}$ NMR(126 MHz, CD_3CN): δ 24.7 (s, $\text{CH}(\text{CH}_3)_2$), 26.0 (s, $\text{CH}(\text{CH}_3)_2$), 29.4 (s, $\text{CH}(\text{CH}_3)_2$), 125.0 (s, Dip-C), 125.2 (d, $^2J_{\text{P,C}}=19.7$ Hz, C6), 125.8 (d, $^3J_{\text{P,C}}=2.9$ Hz, C3), 127.3 (d, $^4J_{\text{P,C}}=1.6$ Hz, C4), 127.7 (d, $^3J_{\text{P,C}}=16.4$ Hz, C5), 131.2 (s, Dip-C), 132.6 (d, $^2J_{\text{P,C}}=5.1$ Hz, C2), 137.2 (d, $^2J_{\text{P,C}}=7.7$ Hz, Dip-C), 146.4 (d, $^2J_{\text{P,C}}=2.2$ Hz, Dip-C), 148.1 (d, $^2J_{\text{P,C}}=8.4$ Hz, C7), 161.5 (d, $^1J_{\text{P,C}}=23.7$ Hz, C1) ppm. $^{11}\text{B}\{^1\text{H}\}$ NMR (128 Hz, CD_3CN): δ -3.8 (s) ppm. $^{19}\text{F}\{^1\text{H}\}$ NMR (376 Hz, CD_3CN): δ -146.4 (s) ppm. $^{31}\text{P}\{^1\text{H}\}$ NMR (162 MHz, CD_3CN): δ 150.8 (s) ppm.

12: The procedure was similar to that described above for **11**. 144 mg (0.49 mmol) of **1** in 5 mL of Et_2O and 125 mg (0.49 mmol) of AgOTf in 5 mL of Et_2O gave **12** as yellow powder. Yield 202 mg (75%), M.p. 171 °C(dec.). Anal. Calcd. for $\text{C}_{20}\text{H}_{22}\text{AgF}_3\text{NO}_3\text{PS}$: C, 43.5; H, 4.0; N, 2.5. Found: C, 43.8; H, 3.6; N, 2.4. ^1H NMR (500 MHz, CD_3CN): δ 1.11 (d, $^3J=6.9$ Hz, 6H, $\text{CH}(\text{CH}_3)_2$), 1.18 (d, $^3J=6.9$ Hz, 6H, $\text{CH}(\text{CH}_3)_2$), 2.27 (sept, $^3J=6.9$ Hz, 2H, $\text{CH}(\text{CH}_3)_2$), 7.38 (m, 4H, H4+H5+Dip-H), 7.52 (t, $^3J=7.8$ Hz, 1H, Dip-H), 8.03 (m, 1H, H3), 8.13 (m, 1H, H6), 8.42 (s, 1H, H7) ppm. $^{13}\text{C}\{^1\text{H}\}$ NMR(126 MHz, CD_3CN): δ 24.8 (s, $\text{CH}(\text{CH}_3)_2$), 25.9 (s, $\text{CH}(\text{CH}_3)_2$), 29.3 (s, $\text{CH}(\text{CH}_3)_2$), 122.2 (q, $^1J_{\text{F,C}}=316$ Hz, CF_3), 125.0 (s, $^2J_{\text{P,C}}=19.8$ Hz, Dip-C), 125.2 (d, $^2J_{\text{P,C}}=19.8$ Hz, C6), 125.6 (d, $^3J_{\text{P,C}}=3.3$ Hz, C3), 127.1 (d, $^4J_{\text{P,C}}=1.6$ Hz, C4), 127.3 (d, $^3J_{\text{P,C}}=17.0$ Hz, C5), 131.1 (s, Dip-C), 132.5 (d, $^2J_{\text{P,C}}=5.4$ Hz, C2), 137.4 (d, $^2J_{\text{P,C}}=7.6$ Hz, Dip-C), 146.4 (d, $^3J_{\text{P,C}}=1.7$ Hz, Dip-C), 146.9 (d, $^2J_{\text{P,C}}=8.5$ Hz, C7), 161.3 (d, $^1J_{\text{P,C}}=25.7$ Hz, C1) ppm. $^{19}\text{F}\{^1\text{H}\}$ NMR (376 Hz, CD_3CN): δ -79.3 (s) ppm. $^{31}\text{P}\{^1\text{H}\}$ NMR (162 MHz, CD_3CN): δ 149.5 (s) ppm.

13: 784 mg (2.65 mmol) of **1** was dissolved in 10 mL of dichloromethane and was added to a solution of $\text{Co}_2(\text{CO})_8$ 906 mg (2.65 mmol). Instantly, the reaction mixture turned deep blue, while producing CO. The reaction mixture was stirred overnight, evaporated, and washed with hexane. Finally, the precipitate was extracted with 5 mL of DCM, layered with several drops of hexane and crystallized at -30 °C giving deep blue crystals of **13**. Yield 1.32 g (86%), M.p. 283 °C. Anal. Calcd. for $\text{C}_{26}\text{H}_{23}\text{Co}_2\text{NO}_6\text{P}$: C, 51.7; H, 3.8; N, 2.4. Found: C, 51.9; H, 3.6; N, 2.5. ^1H NMR (500 MHz, CD_2Cl_2): δ 1.12 (d, $^3J=6.75$ Hz, 6H, $\text{CH}(\text{CH}_3)_2$), 1.31 (d, $^3J=6.75$ Hz, 6H, $\text{CH}(\text{CH}_3)_2$), 2.81 (sept, $^3J=6.75$ Hz, 2H, $\text{CH}(\text{CH}_3)_2$), 7.31 (d, $^3J=7.85$ Hz, 2H, Dip-H), 7.48 (t, $^3J=7.80$ Hz, 1H, Dip-H), 7.79 (m, 1H, H4), 7.88 (m, 1H, H6), 7.91 (m, 1H, H5), 8.31 (d, $^3J=7.95$ Hz, 1H, H3), 9.32 (d, $^4J_{\text{P,H}}=7.0$ Hz, 1H, H7) ppm. $^{13}\text{C}\{^1\text{H}\}$ NMR (126 MHz, CD_2Cl_2): δ 22.2 (s, $\text{CH}(\text{CH}_3)_2$), 28.2 (s, $\text{CH}(\text{CH}_3)_2$), 29.7 (s, $\text{CH}(\text{CH}_3)_2$), 124.8 (s, Dip-C), 128.0 (d, $^3J_{\text{P,C}}=18.7$ Hz, C5), 130.2 (d, $^4J_{\text{P,C}}=2.0$ Hz, C4), 130.6 (d, $^3J_{\text{P,C}}=3.1$ Hz, C3), 131.4 (s, Dip-C), 133.3 (d, $^2J_{\text{P,C}}=2.3$ Hz, C2), 133.8 (d, $^2J_{\text{P,C}}=3.3$ Hz, Dip-C), 134.3 (d, $^2J_{\text{P,C}}=13.49$ Hz, C6), 145.4 (s, Dip-C), 161.2 (d, $^3J_{\text{P,C}}=1.1$ Hz, C1), 166.3 (s, C7), 206.3 (s, CO) ppm. $^{31}\text{P}\{^1\text{H}\}$ NMR (202 MHz, CD_2Cl_2): δ 265.6 (s) ppm. IR [cm^{-1}]: 2043 s, 1998vs, 1987vs, 1961vs, 1951vs, 1932vs. ($\nu_{\text{C=O}}$). IR [toluene, cm^{-1}]: 2046 s, 2005 s, 1978 s ($\nu_{\text{C=O}}$).

X-ray diffraction analysis

Full-sets of diffraction data of studied compounds were collected at 150(2)K with a Bruker D8-Venture diffractometer equipped with Cu ($\text{Cu}/\text{K}\alpha$ radiation; $\lambda=1.54178$ Å) or Mo ($\text{Mo}/\text{K}\alpha$ radiation; $\lambda=0.71073$ Å) microfocus X-ray (μS) sources, Photon CMOS detector and Oxford Cryosystems cooling device was used for data collection. The frames were integrated with the Bruker SAINT software package using a narrow-frame algorithm. Data were corrected for absorption effects using the Multi-Scan method (SADABS). The obtained data were treated by the XT-version 2018/1 and SHELXL-2017/1 software implemented in APEX3 v2016.5-0 (Bruker AXS) system.^[41] Hydrogen atoms were mostly localized on a difference Fourier map, however to ensure the uniformity of the treatment of the crystals, all hydrogen atoms were recalculated into idealized positions (riding model) and assigned temperature factors $H_{\text{iso}}(\text{H})=1.2 U_{\text{eq}}$ (pivot atom) or of $1.5U_{\text{eq}}$ (methyl). H atoms in methyl, methylene, methine and hydrogen atoms in aromatic rings were placed with C–H distances of 0.99, 0.98, 0.97 and 0.95 Å, respectively. The disordered parts of the structures of **6**, **7** and **12** were split to two positions and refined by standard methods implemented in SHELXL software. In cases of **10** and **12**, there are residual peaks of electron density in the proximity of the Ag and Au atoms, which could be caused by structure modulation. Different treatment of these crystals (absorption correction – various types) helped only in a limited manner. There is disordered solvent (n-hexane) in the structure of **2**. Attempts were made to model this disorder or split it into two positions, but were unsuccessful. PLATON/SQUEZZE^[42] was used to correct the data for the presence of disordered solvent. A potential solvent volume of 229 Å³ was found. 35 electrons per unit cell worth of scattering were located in the void. The calculated stoichiometry of solvent was calculated to be one half of the n-hexane molecule per unit cell which results in 25 electrons per unit cell. Deposition Numbers 2041391 (for **2**), 2041393 (for **3**), 2041394 (for **5**), 2041399 (for **6**), 2041392 (for **7**), 2041396 (for **9**), 2041395 (for **10**), 2041398 (for **12**) and 2041397 (for **13**) contain(s) the supplementary crystallographic data for this paper. These data are provided free of charge by the joint Cambridge Crystallographic Data Centre and Fachinformationszentrum Karlsruhe Access Structures service www.ccdc.cam.ac.uk/structures.

Theoretical studies

All the computations were performed using the Gaussian 09 suite of programs.^[43] All structures were optimized using the ω B97XD functional combined with the def2-TZVP basis set. At each of the optimized structures vibrational analysis was performed to check that the stationary point located is a minimum on the potential energy hypersurface (no imaginary frequencies were obtained). The NBO analysis was carried out with the NBO 5.9 program.^[44] The molecular orbitals were plotted with the Avogadro program.^[45] For the atoms in molecules analysis the Multiwfn program was employed.^[46]

Acknowledgements

The authors (L. D.) thank the Czech Science Foundation (no. 18-10222 S). The work was supported by a János Bolyai Research Fellowship, the Új Nemzeti Kiválóság Program ÚNKP-20-5-BME-317, NRDI. Fund (TKP2020 IES, Grant No. BME-IE-NAT) based on the charter of bolster issued by the NRDI Office under the auspices of the Ministry for Innovation and Technology.

Conflict of Interest

The authors declare no conflict of interest.

Keywords: Diels-Alder reactions · heterodienes · NRT study · phospho-heterocycles · phosphinidenes

- [1] For recent review see: a) L. Dostál, *Coord. Chem. Rev.* **2017**, *353*, 142–158.
- [2] M. T. Nguyen, A. van Keer, L. G. Vanquickenborne, *J. Org. Chem.* **1996**, *61*, 7077–7084.
- [3] For relevant examples see: a) S. Shah, M. C. Simpson, R. C. Smith, J. D. Protasiewicz, *J. Am. Chem. Soc.* **2001**, *123*, 6925–6926; b) A. H. Cowley, F. P. Gabbaï, R. Schluter, D. A. Atwood, *J. Am. Chem. Soc.* **1992**, *114*, 3142–3144; c) G. Bucher, M. L. G. Borst, A. W. Ehlers, K. Lammertsma, S. Ceola, M. Huber, D. Grote, W. Sander, *Angew. Chem.* **2005**, *117*, 3353–3357, *Angew. Chem. Int. Ed.* **2005**, *44*, 3289–3293; d) X. Li, D. Lei, M. Y. Chiang, P. P. Gaspar, *J. Am. Chem. Soc.* **1992**, *114*, 8526–8531; e) A. Mardyukov, D. Niedek, P. R. Scheiner, *J. Am. Chem. Soc.* **2017**, *139*, 5019–5022.
- [4] For selected reviews in this rich field see: a) F. Mathey, *Angew. Chem.* **1987**, *99*, 285–296, *Angew. Chem. Int. Ed.* **1987**, *26*, 275–286; b) F. Mathey, *Angew. Chem.* **2003**, *115*, 1616–1643, *Angew. Chem. Int. Ed.* **2003**, *42*, 1578–1604; c) F. Mathey, *Dalton Trans.* **2007**, 1861–1868; d) H. Aktas, J. C. Sloatweg, K. Lammertsma, *Angew. Chem.* **2010**, *122*, 2148–2159, *Angew. Chem. Int. Ed.* **2010**, *49*, 2102–2113; e) K. Lammertsma, *Top. Cur. Chem.* **2003**, *229*, 95–119; f) R. Streubel, *Coord. Chem. Rev.* **2002**, *227*, 175–192; g) M. E. García, D. García-Vivó, A. Ramos, M. A. Ruiz, *Coord. Chem. Rev.* **2017**, *330*, 1–36; h) C. Y. Huang, A. G. Doyle, *Chem. Rev.* **2014**, *114*, 8153–8198.
- [5] a) A. Velian, C. C. Cummins, *J. Am. Chem. Soc.* **2012**, *134*, 13978–13981; b) A. Velian, M. Nava, M. Temprado, Y. Zhou, R. W. Field, C. C. Cummins, *J. Am. Chem. Soc.* **2014**, *136*, 13586–13589; c) W. J. Transue, A. Velian, M. Nava, C. García-Iriepa, M. Temprado, C. C. Cummins, *J. Am. Chem. Soc.* **2017**, *139*, 10822–10831; d) W. J. Transue, M. Nava, M. W. Terban, J. Yang, M. W. Greenberg, G. Wu, E. E. Foreman, C. L. Mustoe, P. Kennepohl, J. S. Owen, S. J. L. Billinge, H. J. Kulik, C. C. Cummins, *J. Am. Chem. Soc.* **2019**, *141*, 431–440; e) K. M. Szkop, M. B. Geeson, D. W. Stephan, C. C. Cummins, *Chem. Sci.* **2019**, *10*, 3627–3631; f) M. B. Geeson, W. J. Transue, C. C. Cummins, *J. Am. Chem. Soc.* **2019**, *141*, 13336–13340.
- [6] Z. Benkő, R. Streubel, L. Nyulázi, *Dalton Trans.* **2006**, 4321–4327.
- [7] L. Liu, D. A. Ruiz, D. Munz, G. Bertrand, *Chem* **2016**, *1*, 147–153.
- [8] For example see: a) M. M. Hansmann, R. Jazzar, G. Bertrand, *J. Am. Chem. Soc.* **2016**, *138*, 8356–8359; M. M. Hansmann, G. Bertrand, *J. Am. Chem. Soc.* **2016**, *138*, 15885–15886.
- [9] A. J. Arduengo, J. C. Calabrese, A. H. Colwey, H. V. Rasika Dias, J. R. Goerlich, W. J. Marshall, R. Riegel, *Inorg. Chem.* **1997**, *36*, 2151–2158.
- [10] a) T. Krachko, J. C. Sloatweg, *Eur. J. Inorg. Chem.* **2018**, 2734–2754; b) V. Nesterov, D. Reiter, P. Bag, P. Frisch, R. Holzner, A. Porzelt, S. Inoue, *Chem. Rev.* **2018**, *118*, 9678–9842; c) A. Doddi, M. Peters, M. Tamm, *Chem. Rev.* **2019**, *119*, 6994–7112; d) O. Back, M. Henry-Ellinger, C. D. Martin, D. Martin, G. Bertrand, *Angew. Chem.* **2013**, *125*, 3011–3015; *Angew. Chem. Int. Ed.* **2013**, *52*, 2939–2943.
- [11] a) P. Šimon, F. De Proft, R. Jambor, A. Růžicka, L. Dostál, *Angew. Chem.* **2010**, *122*, 5600–5603; *Angew. Chem. Int. Ed.* **2010**, *49*, 5468–5471; b) I. Vránová, M. Alonso, R. Lo, R. Sedlák, R. Jambor, A. Růžicka, F. De Proft, P. Hobza, L. Dostál, *Chem. Eur. J.* **2015**, *21*, 16917–16928; c) J. Hývl, W. Y. Yoshida, A. L. Rheingold, R. P. Hughes, M. F. Cain, *Chem. Eur. J.* **2016**, *22*, 17562–17565; d) I. Vránová, M. Alonso, R. Jambor, A. Růžicka, J. Turek, L. Dostál, *Chem. Eur. J.* **2017**, *23*, 2340–2349; e) M. T. Nguyen, B. Gabidullin, G. I. Nikovov, *Dalton Trans.* **2018**, *47*, 17011–17019; f) I. Vránová, M. Alonso, R. Jambor, A. Růžicka, M. Erben, L. Dostál, *Chem. Eur. J.* **2016**, *22*, 7376–7380.
- [12] V. Kremláček, J. Hývl, W. Y. Yoshida, A. Růžicka, A. L. Rheingold, J. Turek, R. P. Hughes, L. Dostál, M. F. Cain, *Organometallics* **2018**, *37*, 2481–2490.
- [13] The titled 2,1-benzazaphosphole has been for the first time prepared as an unexpected product by Tokitoh et al.: N. Tokitoh, T. Matsumoto, T. Sasamori, *Heterocycles* **2008**, *76*, 981–987.
- [14] a) L. Dostál, R. Jambor, A. Růžicka, P. Šimon, *Eur. J. Inorg. Chem.* **2011**, 2380–2386; b) P. Šimon, R. Jambor, A. Růžicka, L. Dostál, *Organometallics* **2013**, *32*, 239–248.
- [15] a) M. Schiffer, M. Scheer, *Angew. Chem.* **2001**, *117*, 3353–3357, *Angew. Chem. Int. Ed.* **2001**, *113*, 3520–3523; this work has been further developed in: b) M. Seidl, R. Weinzierl, A. Y. Timoshkin, M. Scheer, *Chem. Eur. J.* **2016**, *22*, 5484–5488.
- [16] a) M. Kořenková, V. Kremláček, M. Hejda, J. Turek, R. Khudaverdyan, M. Erben, R. Jambor, A. Růžicka, L. Dostál, *Chem. Eur. J.* **2020**, *26*, 1144–1154; b) V. Kremláček, M. Erben, R. Jambor, A. Růžicka, J. Turek, E. Rychagova, S. Ketkov, L. Dostál, *Chem. Eur. J.* **2019**, *25*, 5668–5671.
- [17] M. Ghalib, L. Kőnczöl, L. Nyulázi, P. G. Jones, G. J. Palm, J. W. Heinicke, *Dalton Trans.* **2014**, *43*, 51–54.
- [18] For recent examples of hetero-DA reaction with P-containing dienes see a) M. M. Hansmann, *Chem. Eur. J.* **2018**, *24*, 11573–11577 and references cited therein; b) X. Chen, S. Alidori, F. F. Puschmann, G. Santiso-Quinones, Z. Benkő, Z. Li, G. Becker, H.-F. Grützmacher, H. Grützmacher, *Angew. Chem.* **2014**, *126*, 1667–1671; *Angew. Chem. Int. Ed.* **2014**, *53*, 1641–1645; c) Y. Mao, F. Mathey, *Chem. Eur. J.* **2011**, *17*, 10745–10751; d) Y. Mei, D.-J. Wu, J. E. Borger, H. Grützmacher, *Angew. Chem.* **2018**, *130*, 5610–5613; *Angew. Chem. Int. Ed.* **2018**, *57*, 5512–5515; e) P. Wonneberger, N. König, F. B. Kraft, M. B. Sárosi, E. Hey-Hawkins, *Angew. Chem.* **2018**, *131*, 3240–3244, *Angew. Chem. Int. Ed.* **2018**, *58*, 3208–3211; f) T. Möller, M. Sarosi, E. Hey-Hawkins, *Chem. Eur. J.* **2012**, *18*, 16604–16607; g) T. Möller, P. Wonneberger, N. Kretschmar, E. Hey-Hawkins, *Chem. Commun.* **2014**, *50*, 5826–5828; h) T. Möller, P. Wonneberger, M. B. Sárosi, P. Coburger, E. Hey-Hawkins, *Dalton Trans.* **2016**, *45*, 1904–1917; i) A. Zagidullin, V. Miluykov, F. Poyancev, Sh. Latypov, O. Sinyashin, P. Lönnecke, E. Hey-Hawkins, *Eur. J. Org. Chem.* **2015**, 5326–5329; j) A. Zagidullin, V. Miluykov, D. Krivolapov, S. Kharlamov, Sh. Latypov, O. Sinyashin, P. Lönnecke, E. Hey-Hawkins, *Eur. J. Org. Chem.* **2011**, 4910–4918; k) A. A. Zagidullin, E. S. Oshchepkova, I. V. Chuchelkin, S. A. Kondrashova, V. A. Miluykova, Sh. K. Latypov, K. N. Gavrilov, E. Hey-Hawkins, *Dalton Trans.* **2019**, *48*, 4677–4684 and references cited therein; l) M. Bruce, M. Papke, A. W. Ehlers, M. Weber, D. Lentz, N. Mézailles, J. C. Sloatweg, C. Müller, *Chem. Eur. J.* **2019**, *25*, 14332–14340; m) M. Rigo, M. Weber, C. Müller, *Chem. Commun.* **2016**, *52*, 7090–7093; n) C. Müller, E. A. Pidko, D. Totev, M. Lutz, A. L. Spek, R. A. van Santen, D. Vogt, *Dalton Trans.* **2007**, 5372–5375; o) M. Rigo, E. R. M. Habraken, K. Bhattacharyya, M. Weber, A. W. Ehlers, N. Mézailles, J. C. Sloatweg, C. Müller, *Chem. Eur. J.* **2019**, *25*, 8769–8779.
- [19] Albeit the traces of the alkyne were detected (¹⁹F NMR) even in the bulk sample of **3** that could not be removed even by repeated crystallizations and hampered observation of satisfactory EA data, it could be used for further preparation of **5**.
- [20] P. Pyykkö, M. Atsumi, *Chem. Eur. J.* **2009**, *15*, 186–197.
- [21] P. Pyykkö, M. Atsumi, *Chem. Eur. J.* **2009**, *15*, 12770–12779.
- [22] G. Socrates, *Infrared and Raman Characteristic Group Frequencies: Tables and Charts, 3rd Edition*, John Wiley&Sons LTD, UK, **2004**, 366.

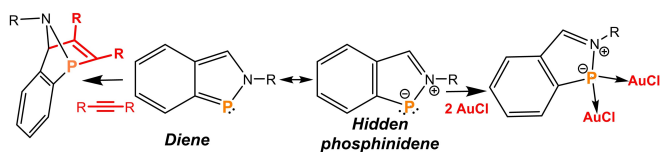
- [23] This approach was motivated by the following work: B. Ritschel, J. Poater, H. Dengel, M. F. Bickelhaupt, C. Lichtenberg, *Angew. Chem.* **2018**, *130*, 3887–3891; *Angew. Chem. Int. Ed.* **2018**, *57*, 3825–3829.
- [24] Albeit a sufficient amount of **6** was obtained for complete NMR and XRD analysis a controlled way for its synthesis is not available at the moment.
- [25] G. Märkl, A. Kallmünzer, *Tetrahedron Lett.* **1992**, *33*, 1597–1600.
- [26] a) A. Moores, T. Cantat, L. Ricard, N. Mézailles, F. Mathey, *New J. Chem.* **2007**, *31*, 1493–1498; b) G. Maas, J. Fink, H. Wingert, K. Blatter, M. Regitz, *Chem. Ber.* **1987**, *120*, 819–824; c) C. Müller, D. Wasserberg, J. J. Weemers, E. A. Pidko, S. Hoffmann, M. Lutz, A. L. Spek, S. C. J. Meskers, R. A. J. Janssen, R. A. van Santen, D. Vogt, *Chem. Eur. J.* **2007**, *13*, 4548–4559; d) H. Onken, J. Lottermoser, *Naturwissenschaften* **1967**, *54*, 560–561; e) M. Bruce, G. Meissner, M. Weber, J. Wiecko, C. Müller, *Eur. J. Inorg. Chem.* **2014**, 1719–1726.
- [27] A. Matsumoto, M. Suzuki, H. Hayashi, D. Kuzuhara, J. Yuasa, T. Kawai, N. Aratani, H. Yamada, *Chem. Eur. J.* **2016**, *22*, 14462–14466.
- [28] a) G. Märkl, K. H. Heier, *Angew. Chem.* **1972**, *84*, 1066–1068; *Angew. Chem. Int. Ed.* **1972**, *11*, 1017–1019.
- [29] T. Posset, F. Rominger, J. Blumel, *Chem. Mater.* **2005**, *17*, 586–595.
- [30] M. Brym, C. Jones, M. Waugh, E. Hey-Hawkins, F. Majoumo, *New J. Chem.* **2003**, *27*, 1614–1621.
- [31] M. Kořenková, M. Hejda, M. Erben, R. Jirásko, R. Jambor, A. Růžička, E. Rychagova, S. Ketkov, L. Dostál, *Chem. Eur. J.* **2019**, *25*, 12884–12888.
- [32] For example see: a) B. A. Surgenor, M. Bühl, A. M. Z. Slawin, J. D. Woollins, P. Kilian, *Angew. Chem.* **2012**, *124*, 10297–10300, *Angew. Chem. Int. Ed.* **2012**, *51*, 10150–10153; b) A. Doddi, D. Bockfeld, A. Nasr, T. Bannenberg, P. G. Jones, M. Tamm, *Chem. Eur. J.* **2015**, *21*, 16178–16189; c) V. A. Adiraju, M. Yousufuddin, H. V. R. Dias, *Dalton Trans.* **2015**, *44*, 4449–4454.
- [33] D. V. Partyka, M. P. Washington, J. B. Updegraff, R. A. Woloszynek, J. D. Protasiewicz, *Angew. Chem.* **2008**, *120*, 7599–7602, *Angew. Chem. Int. Ed.* **2008**, *47*, 7489–7492.
- [34] P. J. Ragoon, C. Graham, C. Millet, A. N. Price, J. Valijus, M. J. Cowley, H. Tuonone, *Chem. Eur. J.* **2017**, *24*, 672–680.
- [35] B. A. Surgenor, K. S. A. Arachchige, A. M. Z. Slawin, J. D. Woollins, M. Bühl, P. Kilian, *Inorg. Chem.* **2014**, *53*, 6856–6866.
- [36] A. Schulz, A. Villinger, A. Westenkirchner, *Inorg. Chem.* **2014**, *53*, 3183–3193.
- [37] S. Gómez-Ruiz, R. Wolf, S. Bauer, H. Bittig, A. Schisler, P. Lönnecke, E. Hey-Hawkins, *Chem. Eur. J.* **2008**, *14*, 4511–4520.
- [38] A. Ziolkowska, S. Brauer, L. Ponikiewski, *Z. Allg. Anorg. Chem.* **2019**, *645*, 949–954.
- [39] A. M. Arif, A. H. Cowley, N. C. Norman, A. G. Orpen, M. Pakulski, *Organometallics* **1988**, *7*, 309–318.
- [40] T. A. Zeidan, S. V. Kovalenko, M. Manoharan, R. J. Clark, I. Ghiviriga, I. V. Alabugin, *J. Am. Chem. Soc.* **2005**, *127*, 4270–4285.
- [41] M. Sheldrick, *Acta Crystallogr.* **2015**, *A71*, 3–8.
- [42] P. van der Sluis, A. L. Spek, *Acta Crystallogr., Sect. A* **1990**, *46*, 194–201.
- [43] M. J. Frisch, G. W. Trucks, H. B. Schlegel, G. E. Scuseria, M. A. Robb, J. R. Cheeseman, G. Scalmani, V. Barone, B. Mennucci, G. A. Petersson, H. Nakatsuji, M. Caricato, X. Li, H. P. Hratchian, A. F. Izmaylov, J. Bloino, G. Zheng, J. L. Sonnenberg, M. Hada, M. Ehara, K. Toyota, R. Fukuda, J. Hasegawa, M. Ishida, T. Nakajima, Y. Honda, O. Kitao, H. Nakai, T. Vreven, J. A. Montgomery, Jr., J. E. Peralta, F. Ogliaro, M. Bearpark, J. J. Heyd, E. Brothers, K. N. Kudin, V. N. Staroverov, R. Kobayashi, J. Normand, K. Raghavachari, A. Rendell, J. C. Burant, S. S. Iyengar, J. Tomasi, M. Cossi, N. Rega, J. M. Millam, M. Klene, J. E. Knox, J. B. Cross, V. Bakken, C. Adamo, J. Jaramillo, R. Gomperts, R. E. Stratmann, O. Yazyev, A. J. Austin, R. Cammi, C. Pomelli, J. W. Ochterski, R. L. Martin, K. Morokuma, V. G. Zakrzewski, G. A. Voth, P. Salvador, J. J. Dannenberg, S. Dapprich, A. D. Daniels, Ö. Farkas, J. B. Foresman, J. V. Ortiz, J. Cioslowski, D. J. Fox, Gaussian 09, Revision A.02, Gaussian, Inc., Wallingford CT. **2009**.
- [44] NBO 5.9. E. D. Glendening, J. K. Badenhoop, A. E. Reed, J. E. Carpenter, J. A. Bohmann, C. M. Morales, F. Weinhold, Theoretical Chemistry Institute, University of Wisconsin, Madison, WI, **2009**, <http://www.chem-wisc.edu/~nbo5>.
- [45] Avogadro, <http://avogadro.cc/>.
- [46] T. Lu, F. Chen, *J. Comput. Chem.* **2012**, *33*, 580–592.

Manuscript received: May 12, 2021

Accepted manuscript online: June 7, 2021

Version of record online: ■■■, ■■■■

FULL PAPER



The dualistic behavior of the titled 2,1-benzazaphosphole, behaving as a heterodiene versus a hidden phosphinidene, has been theoretically predicted based on an NTR analysis. This spectacular feature has been proven chemically as well. Thus, it is

able to participate in hetero-Diels-Alder reactions forming expected heterocycles, but it also serves as a 4e ligand, using two phosphorus electron lone pairs, bridging two transition metals (Au, Ag and Co).

V. Kremláček, Mr. E. Kertész, Prof. Z. Benkő*, M. Erben, R. Jirásko, Prof. A. Růžička, Prof. R. Jambor, Prof. L. Dostál*

1 – 13

Non-conventional Behavior of a 2,1-Benzazaphosphole: Heterodiene or Hidden Phosphinidene?

